Journal of Thermal Analysis and Calorimetry (2022) 147:10177–10206
https://doi.org/10.1007/s10973-022-11247-1

The hydrothermal performance enhancement techniques of corrugated channels: a review

Mohanad A. Alfellag[1] · Hamdi E. Ahmed[1] · Mohammed G. Jehad[1] · Ammar A. Farhan[2]

Received: 5 August 2021 / Accepted: 23 January 2022 / Published online: 24 February 2022
© Akadémiai Kiadó, Budapest, Hungary 2022, corrected publication 2022

Abstract

In the last decades, heat transfer enhancement techniques have been varied and increased rapidly to produce more efficient heat exchange equipment and in turn save energy and cost. One of the effective methods used for augmenting heat transfer is employing corrugations on heat exchanger equipment surfaces. Different applications of using corrugations such as circular and non-circular channels, microchannel heat sink, mini-channel heat sink, and solar air collector have been presented and reviewed in this paper. Researchers investigated various shapes of corrugations along with several corrugation configurations. In addition, using corrugations with other heat transfer enhancement techniques, namely perforations, phase change materials, and nanofluids was discussed. From this overview study, it was found that some research topics are still attractive and need more investigations, while other topics have some limitations either in the application or side effects such as additional pressure drop penalty, further machining costs, more additional material, or more costs for synthesizing the coolants such as nanofluids or sedimentation.

Keywords Enhancement techniques · Hydrothermal performance · Corrugated channels · Compound methods · Solar air collector

Abbreviations

CC	Cross-corrugated plate
CHS	Channel heat sink
SST	Single-structured tube
CST	Cross-structured tube
CTSS	Corrugated trays solar still
CWSS	Corrugated wick solar still
ICT	Interruptions in the corrugated tube
LES	Large Eddy Simulation
MCHS	Microchannel heat sink
MHS	Miniature heat sinks
MWCNT-GA	Gum Arabic-treated multi-walled carbon nanotubes
OPI	Overall performance index
PCM	Phase change material
PEC	Performance evaluation criteria
PF	Performance factor
SAH	Solar air heater
SRTs	Sinusoidal ribbed tubes
VGs	Vortex generators

✉ Mohanad A. Alfellag
mohanadheete@uoanbar.edu.iq

✉ Hamdi E. Ahmed
hamdi.ahmed@uoanbar.edu.iq

[1] Department of Mechanical Engineering, College of Engineering, University of Anbar, Ramadi 31001, Iraq

[2] Department of Energy Engineering, College of Engineering, University of Baghdad, Baghdad 10071, Iraq

Introduction

Passive, active, and compound (passive–active) heat transfer enhancement techniques have been introduced to improve the hydrothermal performance of heat exchangers yielding a lighter mass, the smaller size of the exchanger, and lower in the cost of operation. However, due to the loss of energy and to the demand for small sizes and more economic enhanced heat transfer systems, three techniques have been utilized which are essential in many applications, such as compressed air, exhaust gas, paint, oil refrigerators, evaporators or condensers, heat exchangers for power generation, cooling and air-conditioning, and the industrial heat exchangers in chemical and food industry. One of the simplest methods used for improving the thermal performance of heat exchangers involves deforming the channel surface for forming a corrugated wall [1]. The surface area

modifications or manipulations, which could induce swirls or spirally flowing patterns, have attractive increasing attention. The implementation of corrugation for improving the heat transfer has become interesting recently owing to several advantages such as turbulators, extended surfaces, and roughness. The major role of surface corrugations, which is used widely in heat exchangers, is for augmenting the secondary recirculation flows by inducing the mixing of the flow layers. Moreover, the corrugated surfaces could enhance the heat transfer owing to the mixing of fluids caused by the separations and re-attachments [2].

Miniature heat sinks (MHSs) are powerful devices in the thermal management of mechanical or electronic components. The plate–fin heat sinks are easy in fabrication, simple in structure, and low in cost. In modern electronic or mechanical equipment, efficient thermal management systems are necessary, particularly in critical operating conditions such as high heat fluxes. Generally, the heat transfer enhancement in the mini-channel heat sink (CHS) can be executed either by modifying the channel surface or by improving the thermophysical properties of the coolant [3]. Augmenting the thermophysical coolant properties, such as the thermal conductivity, can enhance the heat transfer rate as well. Therefore, the suspending of solid metallic or nonmetallic nanoparticles to the traditional base fluids (poor thermal conductivity) could enhance the heat dissipation ability of the heat exchangers [4]. Some side effects of using nanofluids such as channel surface abrasion, clogging, sedimentation, and other adverse consequences might take place because of particles aggregation and collisions, which restrict their applications somewhat [5].

Flat-plate solar collectors are one of the most potential engineering applications which are simple and inexpensive technology and promise a remarkable reduction in the buildings' energy consumption [6]. The basic role of the solar collectors is to preheat the ambient air for reducing the heating load of conventional ventilating, heating, and air-conditioning systems during the cold season. Solar collectors are featuring low operation cost, long lifetime, high durability, inexpensive maintenance, and ease of installation. There is a great percentage of people who live in rural areas using traditional coal-fired heating systems, which is inadequate and unfriendly to the environment [7]. In contrast, such conventional solar air heaters have low thermal performance and unsatisfactory for significant heat loss [8].

The heat transfer enhancement technique by impinging jet could significantly enhance the local heat transfer coefficients. It is used in many engineering applications where high thermal dissipation is required [9]. The perforated plate–fin heat exchanger could not increase the heat transfer rate, but also reduce the pressure drop penalty [10].

From the available literature, there is an obvious need to survey the latest progress carried out on how and where the corrugation surfaces have been applied and what are the optimal heat transfer enhancement (positive side) and pressure drop increase (negative side) which were obtained. Therefore, the highlight has been applied to the heat transfer enhancement technique, namely corrugation, and categorized according to the engineering applications such as circular channels, wavy and zigzag channels, converged and diverged ducts, mini- and micro-heat sinks, and solar collectors. Different shapes of corrugation have been scanned. In addition, combined techniques with corrugation such as perforation, phase change materials, and nanofluids are also discussed. The conclusion involves a brief tabulated summary to show what has been investigated right now, and a focus on the research gaps which are still under investigation, not investigated yet, or not comprehensively investigated to draw a future research framework and may be a helpful key for the readers to follow one or more of the incomplete research areas.

Circular-corrugated channel

Helical corrugation

Harleß et al. [11] performed a set of experiments of helically single-start and three-start corrugated tubes for exhaust gas heat exchangers with several geometrical configurations. The researchers have examined the effect of the angle, height, and pitch of the corrugation with Reynolds number (*Re*) ranging from 5000 to 23,000. It was revealed that the R3 criterion, a performance evaluation term based on constant pumping power, was 1.55 obtained with a single-start corrugated tube at a dimensionless corrugation pitch of 0.517 and a dimensionless corrugation height of 0.04.

Helical-corrugated multi-tube heat exchanger investigation is numerically carried out by Wang et al. [12], for Re ranged from 8900 to 89,400. Three kinds of tube arrangements are studied, namely circular, square, and triangle, and also several tube spacings are tested along with different tube spacing. Triangular tube showed the highest hydrothermal performance compared with others for Reynolds number below 40,000. Laohalertdecha and Wongwises [13] investigated experimentally helically copper-corrugated tubes to show the thermal and hydraulic performance of R-134a using different corrugated pitches, and depths were explored with a wide range of *Re* number (30,000–120,000). The results showed that when corrugation pitch and depth increased, the Nusselt number (*Nu*) was augmented. Conversely, the two-phase friction factor was not affected significantly by varying corrugation pitch and depth. They predicted the *Nu* number and the friction factor by developing correlations based on their obtained results. In another similar study, experiments were conducted on a

spirally corrugated tube to evaluate the thermal and hydraulic behavior by Vicente et al., [14]. Water and ethylene glycol were used as coolants for $2000 < Re < 90{,}000$ and Prandtl number (Pr) of $2.5 < \mathrm{Pr} < 100$. The severity index ($\varphi = e^2/(p D_n)$) was taken as a geometric parameter to study the effect of roughness on the flow. As a result, the helically corrugated tube could improve the heat transfer and pressure drop up to 300% and 250%, respectively, in compression with the typical tube. Besides, helically corrugated tubes with high severity index showed better thermal performance at $Re < 10{,}000$. On another hand, a corrugated tube with intermediate severity was the best choice for *Re* ranging between 10,000 and 40,000.

Balla [1] conducted a numerical simulation of a six-start helically corrugated tube, as illustrated in Fig. 1, for evaluating the hydrothermal performance considering the severity index as a main geometric parameter. Consequently, for $\varphi = 0.2796$, the performance evaluation criteria $\left(\mathrm{PEC} = \left(\left(\frac{\mathrm{Nu_e}}{\mathrm{Nu_s}}\right)/\left(\frac{\mathrm{f_e}}{\mathrm{f_s}}\right)^{\frac{1}{3}}\right)\right)$ were 2.6–3.7 for *Re* number range of 700–1300, indicating that the use of helical corrugation tubes could significantly enhance the thermal performance.

Harleß et al. [15] carried out an experimental study on a set of cross-corrugated tubes in order to evaluate the enhancement of heat transfer and friction characteristics. Air was used on the inner side of the tubes, while water was employed as a cooling liquid on the outer side. Corrugation pitch and angle were examined for $5000 < Re < 23{,}000$. The highest R3 criterion was 1.55 with a corrugation height and a corrugation angle of 1.86 mm 38.4°, respectively, while the optimum angle was 38.4°.

Barba et al. [2] explored experimentally the effect of helically corrugated tubes, which are used for the chemical and food industry, on the heat transfer and fluid flow characteristics using ethanol glycol as a working fluid for ranging of Reynolds number of 100–800. The *Nu* number was augmented very sensitively compared with the straight tube, while the friction factor increased up to 2.45. Similarly, Rozzi et al. [16] conducted experiments for studying the effect of corrugated tubes, used in the food industry, on the heat transfer and pressure drop of Newtonian and non-Newtonian fluids. Cloudy orange juice, apricot, whole milk, and apple puree fluids were tested. The results demonstrated that there was no noticeable effect of using corrugations at $Re < 800$. For fully developed turbulent flow, a moderate improvement in heat transfer was obtained but with a high-pressure drop. Also, the enhancement of heat transfer in the heating process was better than in the cooling process.

Spirally corrugated tubes were numerically investigated by Wang et al., [17]. Several corrugation height-to-diameter and pitch-to-diameter ratios were covered to study their effect on the heat transfer and turbulent flow characteristics. The swirl and rotational flow were strengthened by increasing the corrugation height ratio and decreasing the corrugation pitch. By increasing the pitch ratio, the swirl flow was weakened while the rotational flow was strengthened. In addition, the improved rotational flow could decrease the heat transfer and flow resistance performance. The maximum values of the local *Nu* number and friction factor were

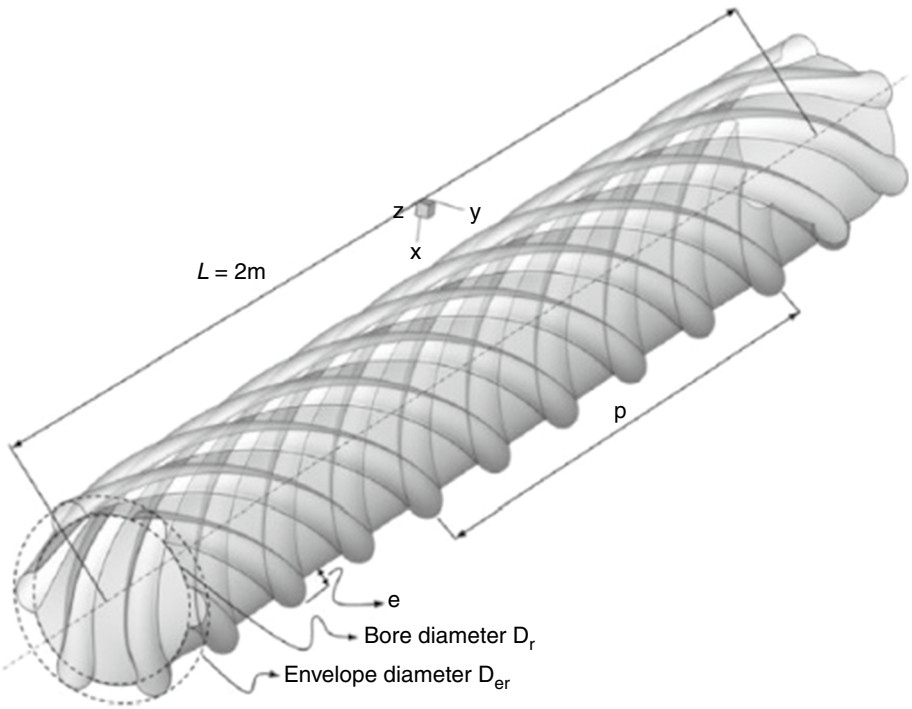

Fig. 1 Six-start spirally corrugated tube [1]

located at the reattachment point, and their minimum values were observed at the center of the swirl flow. They concluded that the height-to-diameter and pitch-to-diameter ratios should be less than 0.1 and 2, respectively, for ensuring that the heat transfer growth rate remains larger than the flow resistance growth rate.

Numerically, Córcoles et al. [18] studied the impact of the helical corrugation of tubes on the turbulent heat transfer and fluid flow characteristics. They pointed out that *Nu* number was augmented by increasing the corrugation height-to-diameter ratio below the ratio of 0.05, while it was decreased with the ratio larger than 0.05. For equal diameter cases, the *Nu* number and pressure drop were both linearly dropped as the pitch to diameter increased. Also, the *Nu* and pressure drop were improved as the height to diameter, severity index, and corrugation shape factor (an indicator of the tube deformation degree) increased.

Xin et al. [19] investigated numerically the heat transfer enhancement and oscillatory flow in a two-start helically corrugated tube with helium as a working medium as shown in Fig. 2. They indicated that the average heat absorption of a two-start spirally corrugated tube was 1.36 times greater than the typical pattern. The performance evaluation criteria (PEC) was 1.38 by average parameters in a cycle, while the value of transient PEC in a cycle was 1.69.

Dong et al. [20] evaluated the heat transfer characteristics and friction factor of four helically corrugated tubes experimentally using water ($6000 < Re < 93{,}000$) and oil ($3200 < Re < 19{,}000$) as coolants with several geometric parameters. The results indicated that the thermal performance of the corrugated tube was higher in comparison with the smooth tube. However, the increase in the friction factor was higher than that in the *Nu* number.

Pethkool et al. [21] investigated experimentally the influence of spiral corrugation on the thermal performance and fluid flow characteristics of the tubular heat exchanger for ($5500 < Re < 60{,}000$) using water as a coolant. Two geometric parameters were considered, namely pitch-to-diameter ratio and rib height-to-diameter ratio. The results revealed that the thermal performance of tubes with spiral corrugation was superior compared to the conventional one. The maximum PEC was 2.3 with a pitch ratio of 0.27 and a rip height ratio of 0.06 at a low *Re* number. They found that the average friction factor of the new design was 1.46–1.93 greater than the smooth tube. Moreover, empirical correlations of *Nu*, *f*, and the thermal performance factor of helically corrugated tubes were derived.

Transverse corrugation

Xiao-Wei et al. [22] investigated experimentally the thermal performance enhancement of roughened tubes for a range of $7000 < Re < 90{,}000$ where the coolant was water. When the corrugation height was lower than the viscous sublayer thickness, the heat transfer was barely augmented. In addition, when the roughness height exceeded the viscous sublayer thickness, heat transfer and flow increased. Moreover, when the corrugation height became five times the viscous sublayer thickness, the friction factor was greatly increased with a small increase in the heat transfer. The thermal performance of corrugated tubes was enhanced employing water with high Prandtl numbers which showed a small pressure drop penalty.

Jaffal et al. [23] numerically performed a numerical study of a transverse-corrugated tube with adding interruptions to the perimeter of the corrugations (ICT), as shown in Fig. 3. The used working fluid was water, and the *Re* was ranged between 1200 and 2240. Several configuration parameters were tested. It was noted that the maximum performance factor achieved is 1.28 at *Re* of 1200. Influence of corrugation width, pitch, and depth of outward convex transverse-corrugated tube was tested and optimized by Lioa et al. [24], in terms of heat transfer and fluid flow characteristics based on roughness parameters of skewness and kurtosis. According to the findings, corrugated tube showed better hydrothermal performance in comparison with smooth tube, and also the hydrothermal performance parameter (PEC) increases with increasing corrugation depth and decreasing corrugation pitch.

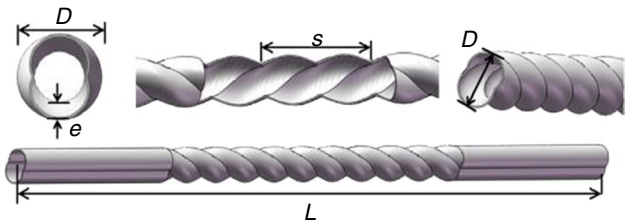

Fig. 2 Structural diagram of the two-start spirally corrugated tube [19]

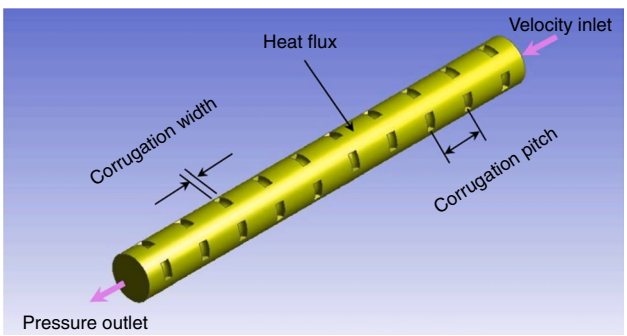

Fig. 3 Computational domain and configurational parameters of the interrupted-corrugated tube [23]

Sun and Zeng [25] performed an experimental and numerical study of three transversely corrugated tubes to determine the thermal and hydraulic characteristics as shown in Fig. 4. The experimental and numerical results revealed that the transversely corrugated tubes could augment the thermal performance by 50% in comparison with the smooth tube; however, the friction factor was increased by more than 50%. They concluded that the transversely corrugated tubes greatly promise effective heat exchange. As a continuous work, a numerical study for a turbulent flow regime was conducted by Mohammed et al., [26]. The rib pitch to diameter, rib width to diameter, and rib height to diameter were optimized. The thermal performance of corrugated tubes was greatly augmented by varying the geometric parameters. The *Nu* was enhanced by increasing the rib height, rib width, and *Re* number and decreasing the rib pitch. The best hydrothermal performance was noticed with rib pitch to diameter, rib width to diameter, and rib height to diameter of 0.5, 0.2, and 0.025, respectively.

Fan et al., [27] performed experiments to study the influence of transversely corrugated tubes on the condensation heat transfer in pure steam and steam–air condition under the turbulent flow regime. In the case of pure steam, they revealed that the condensation heat transfer coefficient of the corrugated tube was increased up to 10% compared with a smooth tube. In the case of steam–air condition, the total pressure of 0.2–0.5 MPa and air mass fraction of 0.1–0.95 were employed to evaluate the condensation heat transfer coefficients.

Experimentally, four transversely corrugated tubes were evaluated by Huang et al. [28], to evaluate the heat and mass transfer performance of falling films. It was found that rib height was the key factor that affected the thermal performance in falling film evaporation. For the same rip pitch and height, the heat transfer was increased when the converging segment of the corrugated tube was longer. They stated that the optimal evaporation mass transfer rate, evaporation heat transfer coefficient, and sensible heating heat transfer coefficient of the corrugated tube were 38%, 62%, and 63%, respectively, higher than the straight tube. For the same corrugated tube, the coefficient of evaporation heat transfer was larger than the coefficient of sensible heating heat transfer. However, both of them were augmented as the flow rate increased.

Fig. 4 Photograph of the corrugated tubes [25]

Non-circular-corrugated channel

Wavy corrugation

Piroozfam et al. [29] investigated computationally the thermal and hydraulic performance of the counterflow heat exchanger using several techniques. One of the applied techniques was a sinusoidal-wavy-corrugated mid-plate between the heat exchanger channels. When the frequency of the sinusoidal-wavy plate increased, the *Nu* number was augmented to a specific value due to an increase in the heat transfer area. However, PEC was reduced with increasing wavy plate frequency, and that was accounted for the increase in the friction factor relative to the increase in *Nu*.

Heat transfer and turbulent flow over a half-wavy-corrugated channel were numerically investigated by Mirzaei et al. [30], employing the large Eddy simulation (LES). Simulations were carried out with a range of normalized wave amplitudes of 0–0.15. It was reported that the wave amplitude strongly affected the recirculating flow region. In addition, as the wave amplitude increased, the *Nu* number was augmented to a specific value and then it remained constant. The optimal thermal performance parameter was 1.19 at a wave amplitude of 0.1. Hydrothermal performance of curved wavy channel was numerically investigated by Zhang et al. [31], under various wave amplitudes, as shown in Fig. 5. Curving the classic wavy channels leads to enhancing the heat transfer rate for several values of amplitudes. For a given dimensionless amplitude, there is an optimal combination of amplitude and wavelength to obtain the highest heat transfer performance. Fluid flow is more sensitive to wavelength.

Tsai et al. [32] investigated experimentally and numerically the pressure drop and distribution flow in two wavy cross-corrugated channels of a plate heat exchanger for $170 < Re < 1700$. The friction factor acted in two different trends considering that *Re* of 430 was the delineating of flow into laminar and turbulent. They indicated that the experimental data of pressure drop was 20% larger than the simulated results.

Faizal and Ahmed [33] performed a set of experiments on a wavy-corrugated plate heat exchanger. Twenty corrugated plates were employed using water for hot and cold channels. Plate spacing of 6, 9, and 12 mm was employed to determine the optimum spacing value. For the same plate spacing, the

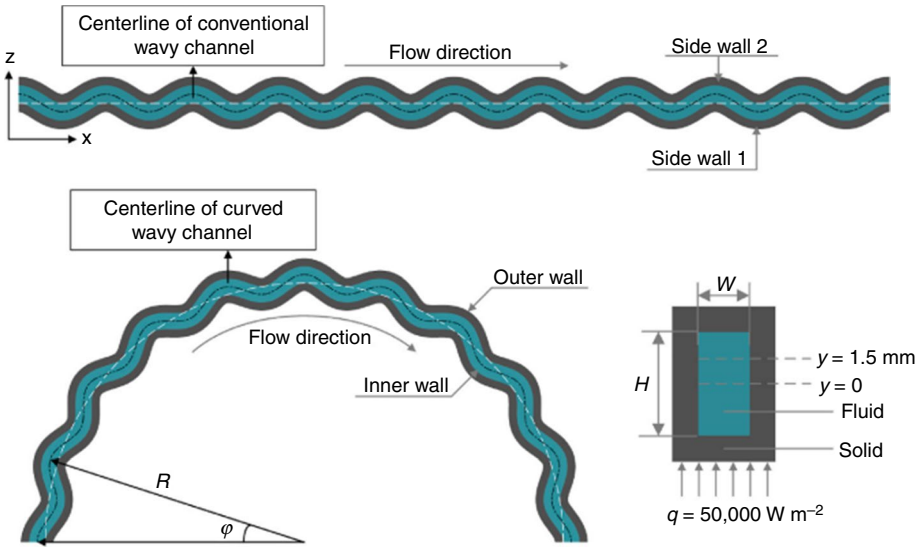

Fig. 5 Schematic diagrams of a conventional wavy channel and a curved wavy channel. [30]

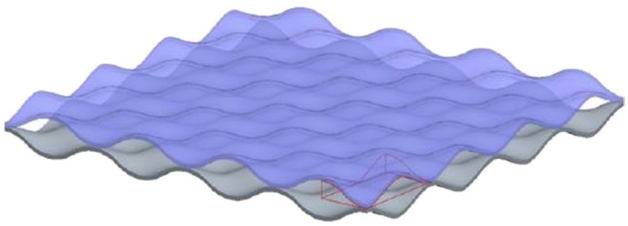

Fig. 6 Offset-bubble primary surface channel [34]

heat exchange between two fluids was augmented when the flow rate of hot water increased because of the corrugation shape which improved the turbulence at high velocity. They pointed out that the optimum spacing which provided a maximum heat transfer was the smallest one.

The hydrothermal behavior of an offset-bubble primary surface channel was proposed by Ma et al., [34]. They adopted the proposed design from the cross-corrugated primary surface channel and offset strip plate–fin channel as shown in Fig. 6. The new design showed better performance than the plate–fin channel and cross-corrugated channel. The area goodness factor (j/f) of the suggested channel was improved by 41% and 71% compared to the previous two channels, respectively. In addition, the wavelength showed a great effect on comprehensive performance compared with wave height.

Hasis et al. [35] studied numerically the geometric variables of a twisted sinusoidal-wavy microchannel for Reynolds number range of $300 < Re < 700$. The ranges of the channel aspect ratio, the waviness, and extent of twist were: 0.5–1.5, 0.03–0.07, and 1–4, respectively. It was reported that the twisted wavy sinusoidal channel showed better performance compared with the wavy sinusoidal channel, and the *Nu* number was augmented with increasing of *Re* number and channel waviness. Heat transfer performance was decreased with decreasing twist extend. However, the channel twisting did not considerably improve heat transfer performance at higher *Re* numbers and the channel waviness. In addition, it was highlighted that the higher aspect ratio means higher heat transfer performance due to the higher asymmetric nature of the flow. The maximum goodness factor achieved was 1.35.

Zigzag corrugation

Naphon [36] studied the impact of zigzag-corrugated channels on heat transfer enhancement under constant heat flux. The proposed modeled channel consisted of two opposite zigzag-corrugated channels as schematically illustrated in Fig. 7. They examined three different tilt angles of 20°, 40°, and 60°. Air was employed as a working fluid for the Reynolds range of 400–1600. They revealed that the *Nu* was augmented with increasing *Re* number. Moreover, the increasing wavy angle showed a better heat transfer rate. As continuous research, another numerical study was performed by Naphon and Kornkumjayrit [37] in which the heat transfer and fluid flow were evaluated using a one-side zigzag-corrugated channel with the tilt angle of 40° and channel height of 7.5 mm. They stated that the corrugated surface had a significant influence on the heat transfer enhancement, and it was a proper method to increase the thermal performance of heat exchangers.

Luo et al. [38] studied the performance of zigzag channel with the implementation of wavy fins and vortex generators (VGs). It is obtained that the longitudinal vortices enhanced the hydrothermal performance compared with smooth wavy channels with a maximum PEC of 1.23. Islamoglu and Parmaksizoglu [39] conducted an experimental study to evaluate the heat transfer coefficients and friction factor using a zigzag-corrugated channel. Experiments were performed

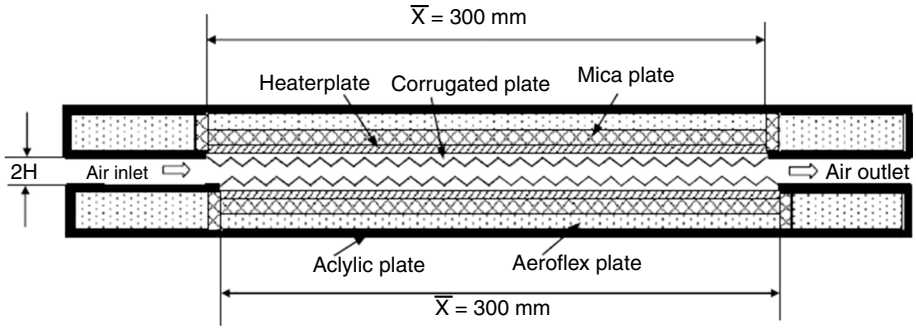

Fig. 7 Schematic diagram of the test section [36]

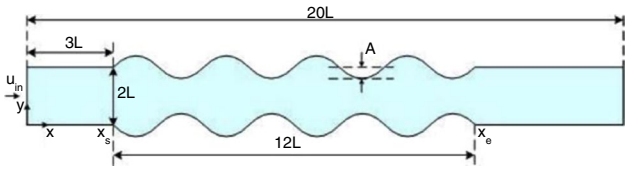

Fig. 8 Schematic diagram of the physical model [42]

with *Re* number range of 1200–4000 with employing air as a coolant. Two different channel heights were considered with a corrugation angle of 20°. As *Re* increased, both the *Nu* number and pressure drop were improved. Moreover, increasing channel height exhibited higher *Nu* number and friction factor.

Mohammed et al. [40] conducted a computational investigation on a zigzag-corrugated channel of a plate heat exchanger to evaluate turbulent convective heat transfer and fluid flow characteristics. The range of *Re* number and heat flux was from 8000 to 20,000 and from 0.4 to 6 kW m^{-2}, respectively, using the working fluid of water. The variable parameters of their study were the corrugation tilt angle, channel height, and wave height. The results indicated that the wavy angle of 20°, channel height of 17.5 mm, and wave height of 2.5 mm were the optimum parameters compared with others, and they showed a great effect on enhancing the thermal performance.

Converging–diverging corrugation

An optimization study of converging–diverging channel under turbulent flow is examined by Parlak et al., [41]. Air was used as a working fluid with Re ranging between 4400 and 6700. The influence of channel width, wavelength, and amplitude has been tested. They stated that the highest hydrothermal performance factor of the optimized channel is 1.7. The hydrothermal performance of non-Newtonian fluid in the converging–diverging corrugated channel, as shown in Fig. 8, was numerically performed by Shubham et al., [42]. Low *Re* number range was covered (10–100), and the power-law index range was 0.6–1.4. The results indicated that the heat transfer enhancement of converging–diverging corrugated channel was noticeable for high wall amplitudes with respect to the smooth channel, while it was insignificant for lower amplitudes, and thermal enhancement was augmented with decrease in the power-law index. Moreover, the heat transfer enhancement ratio of the corrugated channel was more than unity to the corresponding pressure drop ratio for all parameters, so the maximum thermal performance factor (PF) was 0.78. Therefore, selecting converging–diverging corrugated channels for compact heat exchangers using non-Newtonian fluids may lead to significant disadvantages toward the heat transfer effective costs.

In another related study, Wang and Chen [43] investigated numerically the heat transfer rate of fluid flowing inside the converging–diverging corrugated channel. The amplitude–wavelength ratio range was 0–0.5 for $100 < Re < 700$. It was found that with increasing amplitude–wavelength ratio and Reynolds number, the local *Nu* was significantly augmented at the converging section of the wavy wall, while it showed a small increase at the diverging section. Therefore, the larger the amplitude–wavelength ratio, the higher the heat transfer rate, especially at higher *Re*.

Pehlivan [44] investigated experimentally the impact of airflows inside the converging–diverging corrugated channel on convection heat transfer and pressure drop for $2000 < Re < 9000$. Four converging–diverging corrugated channels were tested: two rounded and two sharp corrugation peaks having two different corrugation angles (30° and 50°), two different pitches (8.39 mm and 17.32 mm), and two different channel heights (5 mm and 10 mm). The results revealed that the heat transfer rate was augmented when the *Re* and corrugation angle increased and the channel height and the corrugation pitch decreased. Furthermore, the maximum heat transfer enhancement was about 15 times larger than the straight channel.

Experimentally, Taymaz et al. [45] explored the heat transfer characteristics in a converging–diverging heat exchanger channel using air as a working fluid for $2000 < Re < 7000$. According to their results, the *Nu* was augmented with the increase in the *Re* number and decrease in the channel height. In addition, the converging–diverging

channel showed an increase in heat transfer rate 6 times compared to the straight channel.

Corrugated heat sink

Microscale

Gong et al. [46] optimized numerically the design of wavy microchannel heat sink (MCHS) to show its effect on heat transfer and fluid flow characteristics for low *Re* range, 50–150. Several geometric parameters were the wave amplitude, wavelength, and aspect ratio. Two wavy channel configurations were considered, namely converging–diverging wall and serpentine wall. It was pointed out that the wavy walls showed higher heat transfer augmentation compared to the typical one. Also, the serpentine wall outperformed the converging–diverging walls in terms of thermal performance. The maximum PEC was 1.55 for serpentine wall MCHS. Pourhammati and Hossainpour [47] numerically studied the effect of varying the wave amplitude and wavelength on the hydrothermal performance of the wavy microchannel heat sink (MCHS) under laminar flow. A maximum overall performance (PEC) of 1.338 is achieved.

Rostami et al. [48] carried out a numerical study to determine the optimal design of wavy MCHS employing water as a working fluid. The wall thickness, aspect ratio, amplitude, and wavelength were the key parameters varied in their study with $50 < Re < 200$. According to their results, using wavy MCHS could augment the heat transfer compared to the conventional one. The heat transfer rate was augmented as *Re* and wave amplitude increased due to the presence of secondary flows and recirculation regions. Also, the *Nu* was increased with increasing wall thickness to a certain point and then it started to decrease; however, the pressure drop was decreased as the wall thickness increased.

Numerical research was conducted by Mohammed et al. [49], in which the heat transfer and fluid flow behavior of wavy MCHS were evaluated for $100 < Re < 1000$ and dimensionless wave amplitudes (0.0625–0.25). They indicated that the thermal performance of wavy MCHS was higher than the straight one. Also, it was mentioned that as the wave amplitude ratio increased, the temperature of wavy MCHS, heat transfer coefficient, and pressure drop were increased too. The wave amplitude in the range of 0.0625–0.21875 could lead to optimum thermal performance. Continuously, Mohammed et al. [50] modeled numerically a 3D heat transfer and fluid flow of MCHS considering several channel shapes (i.e., zigzag, curvy, and step) having the same cross section. It was displayed that the heat transfer coefficient and temperature of the zigzag MCHS were the smallest and highest, respectively, relative to other shapes. Additional pressure drop was observed for all channel shapes in comparison with conventional channels. The maximum pressure drop was recorded with the zigzag MCHS followed by the curvy and then step MCHS.

Yong and Teo [51] carried out a numerical investigation on thermal and hydraulic characteristics of converging–diverging MCHS for $50 < Re < 200$ using water as a coolant. The influence of the aspect ratio and amplitude ratio on respective flow behavior and recirculating vortices was examined. The range of the aspect ratio was 0.25–2, and the amplitude ratio was 0.023–0.075. They indicated that the performance of converging–diverging MCHS was superior compared to the straight model. The channel with the aspect ratio range of 0.5–0.1 provided high hydrothermal performance. Moreover, the optimum amplitude ratio range was 0.023–0.035, and when the amplitude ratio increased above the value of 0.035, the hydrothermal performance became almost constant. The maximum achieved PEC was 1.6.

Wan et al. [52] studied computationally and experimentally the impact of half-corrugated MCHS on heat transfer performance and water flow by varying the wave amplitude and wavelength. It was monitored that at lower *Re*, the pressure drop was lower than straight MCHS, and this difference became larger at higher *Re*. The wavelength showed a large impact on the pressure drop compared to the wave amplitude. Furthermore, the *Nu* was augmented with increasing *Re*. The researchers also carried out a comparison with the literature, and they have found that the overall performance of their study was higher than what was obtained by Ref. [104] which employed double-corrugated MCHS.

In another experimental study, Sui et al. [53] investigated the heat transfer and fluid flow in wavy-corrugated MCHS by varying the wave amplitude for $300 < Re < 800$ and using cooling by water. The wavy-corrugated MCHS provided better thermal performance compared with straight MCHS accompanied by an increase in the pressure drop penalty. In addition, the heat transfer and pressure drop were improved with increasing *Re* and wave amplitude. At $Re = 800$ and a wave amplitude of 259 μ m, the maximum heat transfer enhancement was 211%, while the pressure drop was raised to 76% compared to the straight MCHS.

Ermagan and Rafee [54] studied numerically the hydrothermal performance of wavy MCHS with superhydrophobic walls, as graphically illustrated in Fig. 9, for several values of wave amplitude, wavelength, and *Re*. It was mentioned that the *Nu* and pressure drop were augmented with increasing wave amplitude and *Re* number, and decreasing the wavelength. The overall performance was slightly decreased with increasing of *Re*, and the optimum wave amplitude ratio and wavelength ratio were 0.4 and 0.025, respectively. Furthermore, the maximum area goodness factor was 1.47 employing superhydrophobic walls.

A new design of wavy MCHS was proposed by Lin et al. [55], by changing the wavelength and/or wave amplitude

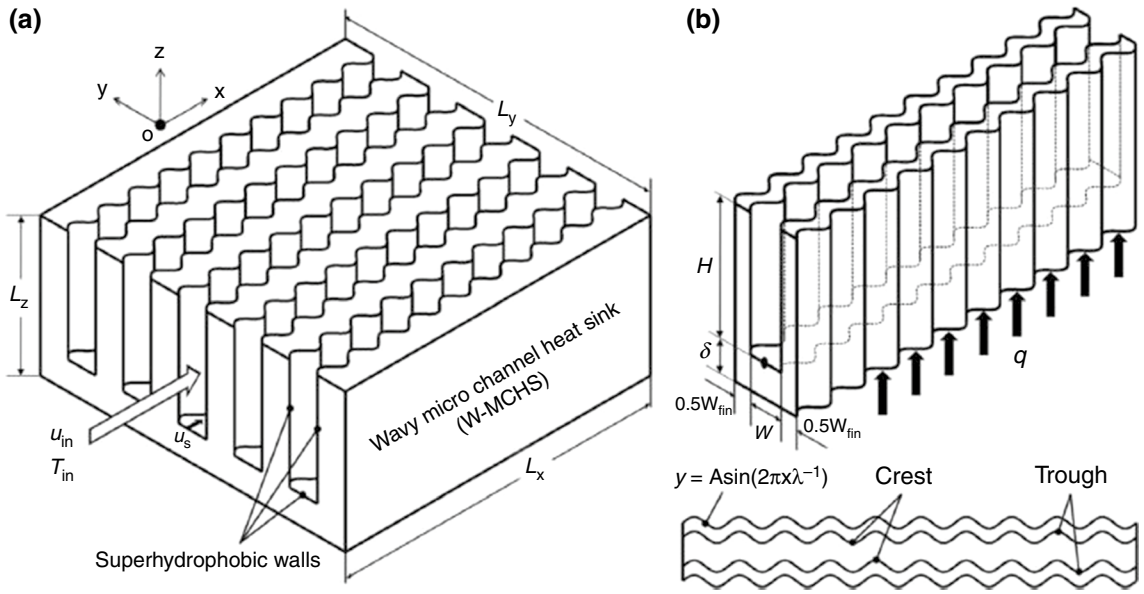

Fig. 9 Schematic of **a** the wavy MCHS with superhydrophobic walls, and **b** coolant sinusoidal flow path [54]

along with flow direction as observed from Fig. 10. The numerical results indicated that the proposed design exhibited greater thermal performance than the conventional wavy as well as the straight MCHS. It was reported that the wavy MCHS with increasing the wave amplitude or decreasing the wavelength along the flow direction showed lower thermal resistance and temperature difference at the bottom surface. Also, for increasing the wave amplitude difference or wavelength difference between two adjacent wavy units, the thermal performance of the proposed design has become more remarkable.

Chiam et al. [56] investigated experimentally and numerically the heat transfer and fluid flow behavior in a wavy MCHS with secondary branches with a range of $50 < Re < 200$ and waviness amplitudes of 0.075 and 0.15. It was highlighted that the effect of secondary branches was more beneficial at $Re < 100$. By adding secondary branches with amplitudes of the waviness of 0.15, the heat transfer performance and pressure drop were both improved with respect to the typical pattern. However, the heat transfer performance was increased with a small increase in pressure drop penalty when the wave amplitude was less than 0.075, whereas the maximum performance factor ($PF = \left(\frac{Nu}{f}/\frac{Nu_s}{f_s}\right)$) was 1.9.

Mini-scale

Khoshvaght-Aliabadi et al. [57] performed a numerical and experimental study to improve the hydrothermal performance of corrugated mini-channel heat sink by changing the cross section size of the routes. Water is used as a working fluid with Re ranging from 85 to 1145. Several models tested including convergent, divergent, and other hybrid models are investigated and compared to the classic design. Results indicated that the divergent model is the best in terms of overall performance index (OPI). Aliabadi and Nozan [58] investigated experimentally the impact of triangular-, sinusoidal-, and trapezoidal-corrugated mini-channel heat sink (mini-CHS) on the heat transfer and pressure

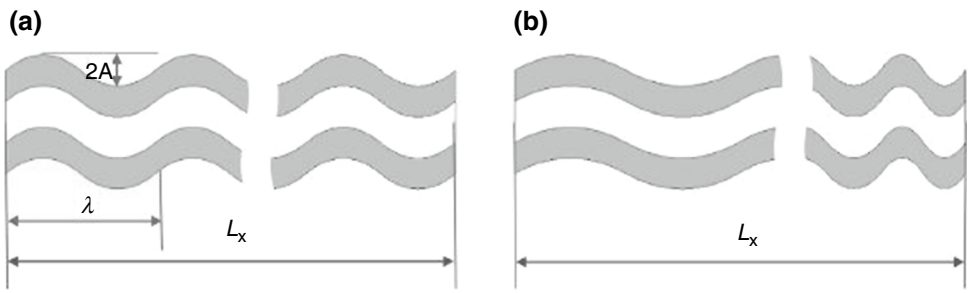

Fig. 10 Top view of the wavy channel: **a** traditional one, and **b** proposed pattern [55]

drop characteristics with varying the corrugation length and corrugation amplitude. By using water as a coolant and $650 < Re < 3000$, it was displayed that the trapezoidal pattern showed higher heat transfer and pumping power compared to others. In addition, when corrugation length decreased and corrugation amplitude increased, both the *Nu* and pumping power were increased. The highest performance factor (the heat transfer to pumping power) was achieved with a sinusoidal pattern having a corrugation length of 30 mm, and a corrugation amplitude of 0.5 mm.

The hydrothermal performance of corrugated mini-CHS cooled by Al_2O_3–water nanofluid was experimentally carried out by Aliabadi and Sahamiyan [59] by varying the parameters of wavelength, wave amplitude, nanoparticles concentration, and mass flow rate. The researchers have obtained higher performance more than that of a straight one. The heat transfer and pressure drop were both raised when the wavelength decreased and/or the wave amplitude increased. The impact of the wavelength was less than that of wave amplitude. The nanofluid showed thermal superiority particularly when the volume fraction increased. Maximum PEC obtained was 3.5 at 0.3 vol.%, the wavelength of 20 mm, the wave amplitude of 2 mm, and the mass flow-rate of 0.024 kg s^{-1}. By using the same coolant, Aliabadi et al. [60] investigated experimentally and numerically the hydrothermal performance wavy mini-CHS with integral and interrupted pin–fins under laminar flow conditions. They found that the pin–fin interrupted wavy heat sink showed higher hydrothermal performance in comparison with the integral pin–fin heat sink. Moreover, the *Nu* and pressure drop were improved when the nanofluid was used instead of water. The highest obtained performance factor was 2.65 at 0.4vol.%. Moreover, the measurements of Aliabadi et al. [61] showed that the sinusoidal-wavy mini-CHS, as illustrated in Fig. 11, provided higher thermal performance when the *Re* ranged from 60–4000 and water–ethylene was used for cooling. They also confirmed that both heat transfer and pressure drop increased as the wave amplitude increased and wavelength decreased. Pure water exhibited a considerable enhancement in heat transfer coefficient compared to the water–ethylene mixture. The maximum heat transfer enhancement obtained was about 200% at the wavelength of 20 mm and wave amplitude of 2 mm, while the optimum geometric design of wavy mini-CHS was for the wavelength of 40 mm and wave amplitude of 1 mm which provided high heat transfer-to-pumping power ratio.

Khalifa and Jaffal [62] studied experimentally and numerically the hydrothermal performance enhancement of corrugated cylindrical mini-CHS for the laminar flow regime as shown in Fig. 12. The corrugation geometry (wavy and helical), aspect ratio, pitch ratio, wave amplitude ratio, and solid void fraction were the variable parameters. In general, corrugated mini-CHS outperformed thermally better than the smooth one. The optimum solid void fraction, aspect ratio, amplitude ratio, and aspect ratio were 0.9, 0.46 0.08, and 2.1, respectively. Also, the *Nu* and pressure drop were both augmented with increasing amplitude and pitch ratios. Highest PEC obtained was 1.16 with the helical corrugation.

Corrugated solar collector

Greig et al. [7] performed an experimental study on the turbulent flow structure in a corrugated surface channel. A remarkable impact of the corrugation waveform was displayed on the flow behavior. The corrugated wall created a complex 3D flow behavior that expanded over the whole channel. The velocity profile exhibited a powerful diffusion of shear. The profile of turbulent properties showed enhanced turbulence in the vicinity of the waveform. The

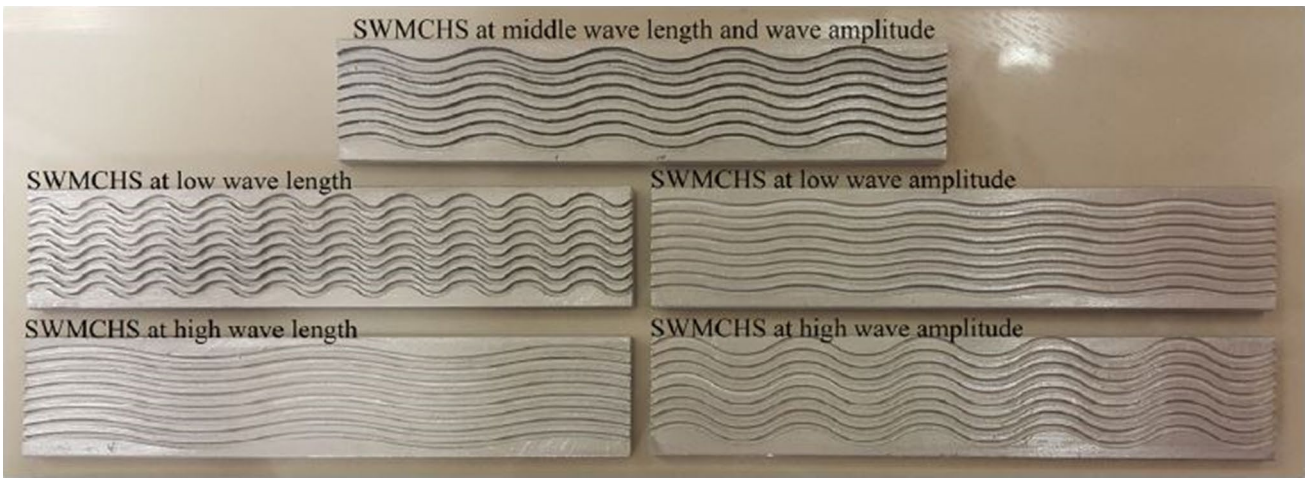

Fig. 11 Top view of fabricated sinusoidal–wavy minichannel heat sink [61]

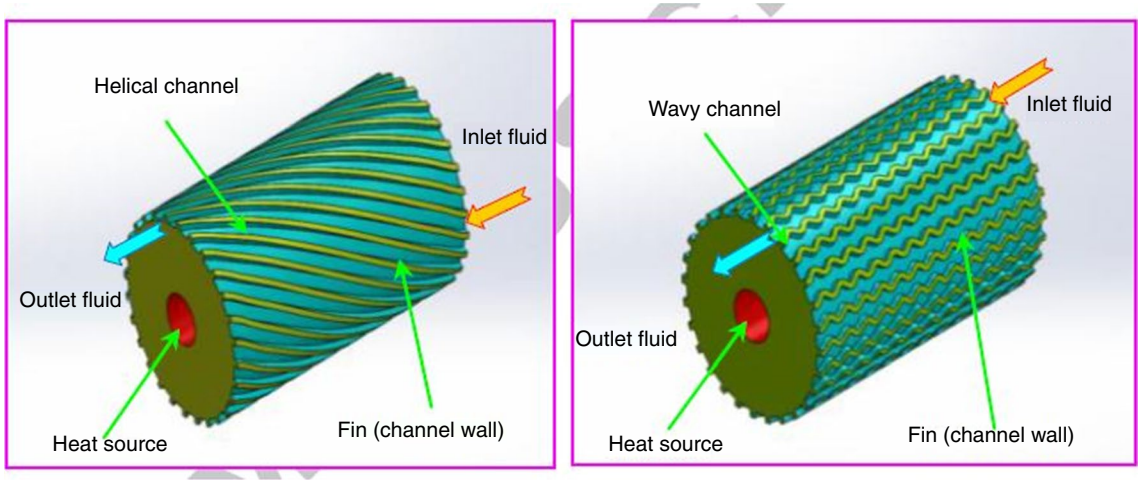

Fig. 12 Helical- and wavy-corrugated minichannel heat sink [62]

turbulence of the flow was almost generated in this region above the corrugated trough. A considerable momentum transfer was monitored from the corrugated surface by the turbulent velocity field. The turbulent flow behavior was periodic compared to the waveform over the channel length. They reported that the existence of intensive turbulence is observed in the laminar flow regime.

An experimental investigation was performed by Abdullah et al. [63], to improve the performance of trays solar still. Three different trays solar still designs are investigated: flat trays solar still, corrugated trays solar still, and conventional solar still. As an additional enhancement, phase change material (PCM) mixed with CuO nanoparticles has been used. According to the results, the total freshwater yield of corrugated trays solar still (CTSS) was increased by 122% using PCM with CuO nanoparticles compared to conventional solar still. In another related study, tilted wick solar stills with different absorber configurations have been tested and evaluated experimentally and theoretically by Younes et al., [64]. Four solar stills designs are built including flat, corrugated, half barrel, and conventional solar stills. It was found that the daily productivity for corrugated wick solar still (CWSS) is improved by 134% in comparison with the conventional solar still.

Aboghrara et al. [65] explored experimentally the outlet temperature and efficiency of corrugated plate solar air heater using circular jet impingement. Their results showed that the flow jet impingement on corrugated plat absorber was a powerful function of thermal augmentation. They observed a substantial influence of the airflow rate on the heat transfer rate. The optimal thermal efficiency of their proposed design rig was about 14% higher than the smooth duct with a temperature increase of up to 3 K.

Taha and Farhan [66] implemented an experimental work to investigate the hydrothermal performance of a solar air collector having zigzag metal foam fins. Fins were attached below the absorbing plate to create five herringbone channels for air flowing. The influence of different corrugated angles on hydrothermal efficiency was studied. Experiments were carried out under outdoor conditions in Iraq during the winter season. They reported that the corrugated angle of 30° gave the highest thermal and hydrothermal efficiencies were 87.7% and 80.2%, respectively, at 0.04 $m^3\ s^{-1}$ airflow rate.

Dormohammadi et al. [67] studied numerically the heat transfer, fluid flow, and entropy generation in a sinusoidal-wavy-wall channel using Cu–water nanofluid coolant. They evaluated the parameters such as nanoparticles concentration (0–5 vol.%), Richardson number ($0.1 < Ri < 10$), wave amplitude, and wavelength. An increase in the *Nu* was recorded with increasing nanoparticle concentration. The highest entropy generation was at a higher Richardson number. The authors could enhance the heat transfer by optimizing the wave amplitude and wavelength parameter.

Pavlovic et al. [68] utilized nanofluids (Al_2O_3, Cu, CuO, and TiO_2 suspended in oil and water base fluid) in a solar dish collector with a smooth and corrugated absorber tube in order to reduce the utilization of traditional energy sources. It was reported that the oil-based nanofluids caused higher exergetic efficiency. However, using water-based nanofluids caused higher thermal performance. The Cu nanoparticle showed the greatest exergetical efficiency among the others, and the maximum exergetic efficiency was up to 12.29% for the Cu–oil-based nanofluid flowing in the corrugated absorber.

Theoretically, Kumar and Chand [69] enhanced the solar air collector performance by using herringbone-corrugated fins attached below the absorber plate along the flow passage. They stated that the optimal air mass flow rate was 0.05 kg s^{-1} which showed maximum thermal efficiency as

there was no significant increase in the efficiency beyond this value. This efficiency increased when the fin pitch decreased owing to the increase in the heat transfer surface area. The maximum efficiency obtained was around 77% at a mass flow rate of 0.08 kg s^{-1} when the corrugated fins were used at a fin pitch of 1 cm. As a comparison with the typical solar collector, the thermal efficiency was improved around 20% when the fins were used accompanied by a penalty of increased pressure drop.

Zheng et al. [70] developed mathematically and experimentally a new solar air collector with metal-corrugated packing for heating buildings in cold regions. It was reported that the ranges of the temperature difference across the collector were 2.95–49.87 K, the thermal efficiency was 47–66%, and the net exergy efficiency of the collector was 0.51–7.31%. Their suggested design was more efficient for heating rural buildings in cold regions due to its great heat transfer area, high convection heat transfer coefficient, and good economic indication. They stated that the thermal efficiency of the collector was increased by increasing the corrugated packing height, specific surface area, radiation intensity, air velocity, and ambient air temperature. On the contrary, it was decreased with increasing the corrugated packing width and air inlet temperature. In addition, their suggested design had lower life-cycle costs and energy-saving potential in the cold rural regions compared to the coal-fired heating system.

Álvarez et al. [71] evaluated the thermal performance of corrugated parallel-plate solar thermal collectors by proposing a new design. A greater thermal performance was recorded for their proposed design compared to the commercial designs. The maximum thermal efficiency they obtained was 86%, whereas it was 80% for the Brown Boveri Corporation product and 77.9% for the Roth Werke product collectors.

Joudi and Farhan [72] investigated experimentally the use of a v-corrugation solar air collector to heat an innovative greenhouse in Iraq during the winter season. A bank of solar air collectors was installed on the roof of the greenhouse. Experiments were implemented to study the effect of different air mass fluxes on the thermal performance of the solar collector under realistic weather conditions. Results show that, to keep the temperature inside the greenhouse at 18 °C, the solar air collectors could be offered about 84% of the daily heating load demand. It was concluded that, at 0.015 kg s^{-1} m^{-2} air mass flux, 45% of the daily heating demand inside greenhouse can be covered.

Kumar et al. [73] carried out experiments on v-corrugated surface solar air heater under laminar flow conditions. The inner surface of the absorber plate was roughened by a shot blasting process. It was declined that the *Nu* was higher for their modified pattern compared to the conventional one, whereas the friction factor was also higher but slightly. The highest thermal efficiency they obtained was around 55% at 0.02 kg s^{-1} for the new pattern. The thermal performance factor decreased with the increase in *Re,* and the greatest value obtained was 1.57 at $Re = 1000$.

Zhang et al. [74] developed the traditional liquid solar collector by using a flat-plate solar collector with dual function. Three modes of heating were studied: air heating, water heating, and air–water compound heating. Their experimental results revealed that the thermal efficiency of the first and second modes was 51.3% and 51.4% at the mass flow rate of 0.024 kg s^{-1} and 0.13 kg s^{-1}, respectively. The maximum air and water temperature obtained was 60.4 °C and 59.8 °C for the respective two modes. Moreover, the thermal efficiency of the last mode was 73.4% greater than the others. The mass flow rate was the major effective factor affecting the efficiency, outlet fluid temperature, and heat transfer rate. For the water flow rate of over 0.10 kg s^{-1}, the heat removal was increased inconsiderably.

Hedayatizadeh et al. [75] paid investigational attention to the v-corrugated solar air heater with various artificial roughness geometries from the exergetic point of view. Their theoretical results showed that as the inlet air temperature was low, the maximum exergy output was achieved with low values of air mass flow rates. But when the inlet air temperature was high, the exergy output increased with the mass flow rate to reach its peak value. The high aspect ratio of the collector could cause an increase in energy and exergy. Low possible triangular ducts bring about a decrease in energy and exergy outputs. They highlighted that a greater number of glasses cover enhanced the exergy outputs, but the economical aspect must be considered in the account.

Double-pass flat and v-corrugated plate solar air heaters were theoretically and experimentally studied by El-Sebaii et al. [8], under the weather conditions of Tanta prevailing—Egypt, as schematically illustrated in Fig. 13. Their results indicated that the double-pass v-corrugated plate model showed an efficiency of about 11–14% higher than the flat mode. The outlet temperature of the v-corrugated plate model was 5% over the typical one. The thermo-hydraulic efficiency of both models was increased with increasing the flow rate until 0.02 kg s^{-1}, and it was decreased remarkably over this flow rate value. Basically, the pressure drop in the case of the v-corrugation pattern was observed higher than the flat plate.

Ho et al., [76] developed theoretically and experimentally a new design of recycling double-pass solar air collector using a v-corrugated absorber. They could enhance the turbulence intensity and convection heat transfer coefficient compared to the conventional flat-plate system. The thermal efficiency was augmented as the airflow rate increased.

Hedayatizadeh et al., [77] analyzed the exergy of double-pass/glazed v-corrugated plate solar air heater based. It was reported that the maximum exergy efficiency of the proposed

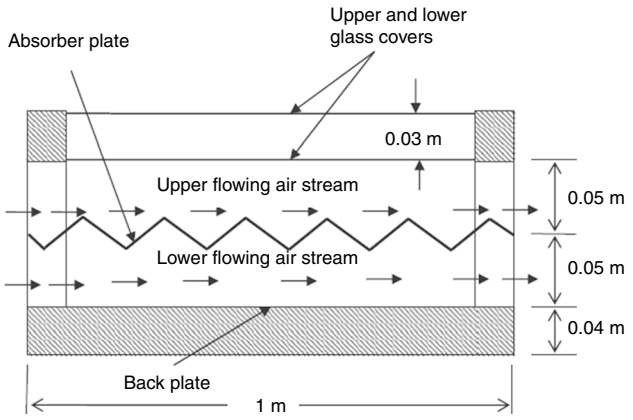

Fig. 13 Scheme of the double-pass v-corrugated plate solar air heater [8]

collector was 6.27% when the distance between the glazings was equal to 2.3 mm, corrugation height of 12.2 mm, heater area of 1.79 m^2, and an airflow rate of 0.005 kg s^{-1}. It was also discovered that the internal exergy loss term originating from the temperature difference between sun and absorber surface was the most fatal term in comparison with the other terms studied in their paper which was 63.57% of the whole exergy losses.

Karim and Hawlader [78] explored experimentally and theoretically the flat-plate, finned and v-corrugated solar air collectors under the climatic conditions of Singapore and over a wide range of design and operating conditions. The collectors were also examined in double-pass mode for showing their effectiveness without the need to increase their size and consequently the cost. Their results demonstrated that the v-corrugated heater was the most efficient mode, whereas the opposite was found with the flat-plate mode. By using double-pass flow, the efficiency of the v-groove mode was 2–5% greater than the finned one and 5–11% greater than the flat-plate one. The double-pass operation of the collector could enhance the efficiency of all proposed patterns. The double-pass mode was most substantial in the flat-plate heater, while it was the waste in the v-groove heater. The efficiency of three collector modes increased with increasing the flow rate until 0.06 kg s^{-1}, as there was no change observed over this value. We would attract the attention of researchers that the authors did not take the pressure drop across the collectors into accounts as they believe that the pressure drop penalty across the v-corrugated and finned solar heater would be higher than the conventional one.

Farhan et al., [79] studied numerically the energetic and exergetic efficiencies of a v-corrugation solar collector having twisted tape inserts inside the airflow channels. They examined the effect of channel numbers and twisted ratio on the hydrothermal performance of the collector with *Re* ranging between 1000 and 20,000. It was reported that when the twisted ratio decreases, the hydrothermal performance of the collector was increasing to the highest value at a certain *Re* value and then decreasing. The maximum hydrothermal performance was found at channel number 5. Results demonstrated that the thermal efficiency of a solar collector with a twisted tape insert was greater than that without a twisted tape insert by about 17.5%.

Configuration of corrugation

Liu et al., [80] perform a comparative study of heat transfer improvement of cross-corrugated and v-corrugated solar air collectors. The study was carried out under a wide range of geometrical and operational conditions. In the case of the cross-corrugated collector, airflow channel was designed by a wavy absorber plate and a wavy bottom plate, while a v-corrugated absorber plate with a flat bottom plate was employed in the case of the v-corrugated collector. The use of the wavy bottom plate in a cross-corrugated collector was to improve the heat transfer rate inside the airflow channel and in turn enhance thermal performance. It was pointed out that the thermal performance of a cross-corrugated collector was higher than the v-corrugated collector in all studied cases. In addition, the thermal performance was augmented with a smaller gap between the cover plate and absorbing plate, slender configuration along the direction of airflow, using a coating on the absorber plate and glass cover that has high solar radiation absorptivity with small thermal radiation emissivity, air mass flow rate above 0.1 kg m^{-2} s^{-1}, and maintaining the temperature of the inlet fluid close to the ambient temperature. The maximum cross-corrugated solar collector efficiency achieved was about 78%, while it was about 69% in the case of the v-corrugated solar collector.

Akbarzadeh et al., [81] numerically investigated the hydrothermal performance of solar air heater with sinusoidal- and triangular-corrugated plates. The proposed study also examined the influence of using Cu–water as the working fluid covering a range of *Re* of 4000–6000. It was reported that hydrothermal performance decreased with increasing *Re* in all cases, and thermal performance and pressure drop were increased when employing a triangular-corrugated plate compared with a sinusoidal one. The hydrothermal performance of corrugated plates was higher than the straight plate using nanofluid. However, employing pure water, the hydrothermal performance of straight plate was higher in comparison with corrugated plates. In addition, increasing nanoparticle concentration of Cu from 0 to 0.04 led to augmenting of PEC reaching a maximum enhancement of 72.4% and 70% for sinusoidal and triangular plates, respectively.

An experimental study was performed by Rainieri and Pagliarini [82] to compare helical- and transverse-corrugated tubes in terms of thermal performance. Experiments were carried out with several pitch values covering a range of *Re* of 90–800 and employing ethylene glycol as the test fluid. It was indicated that the spiral corrugation produced noticeable swirl components, but there was no significant associated heat transfer enhancement, and local *Nu* depended on the corrugated pitch. Also, they pointed out that transverse-corrugated tubes enhanced heat transfer rate higher than helical ones although the helical corrugation is preferable compared with axial symmetrical ones because it is easy to fabricate on a large scale.

In another experimental study, Islamoglu [83] investigated the influence of rounding of protruding edge on thermal performance in the converging–diverging channel as shown in Fig. 14. Experiments were carried out in the *Re* range of 2000–5000 with the angle of the corrugation of 30° and channel height of 5 mm. It was reported that the heat transfer enhancement ratio of sharp corrugation peak was higher than the rounded one about 18% for Re < 3500. As *Re* increased above 3500, the enhancement ratio of rounded corrugation peak became higher than the sharp one with 21%. Furthermore, in terms of flow area goodness factor *(j/f)*, it was revealed that channel with a rounded corrugation peak performed better than that with a sharp corrugation peak in all *Re* numbers.

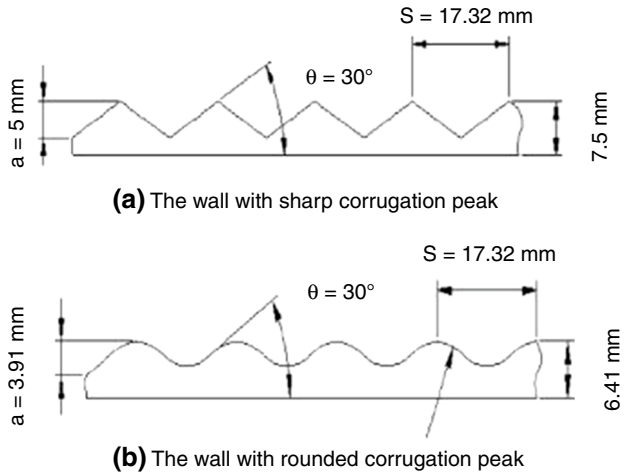

Fig. 14 **a** Triangular- and **b** sinusoidal-corrugated channel [83]

Nelly et al. [84] carried out an experimental investigation on heat transfer and pressure drop behavior of helically single-structured and cross-structured tubes as shown in Fig. 15. Different structure depths and angles were investigated. It was reported that *Nu* and pressure drop ratios were increased with increasing *Re* and structure depth for both tubes. When the structure angle was increased, the *Nu* enhancement ratio was decreased in the case of SSTs, while it increases in CSTs case. In terms of hydrothermal performance, performances of CSTs tubes were higher than SSTs tubes in all cases, and the best structure depths and angles were found to be 0.7 mm and 9°.

The hydrothermal performance of a double-pipe heat exchanger made of inner and outer corrugated tubes was experimentally investigated by Dizaji et al. [85] for $3500 < Re < 18{,}000$. The idea of the proposed study was to compare a double-pipe heat exchanger made of the corrugated inner pipe and straight outer pipe with that made of inner and outer corrugated pipes. Also, they examined the arrangement of concave and convex corrugated pipes as shown in Fig. 16. It was indicated that corrugated pipes improved thermal performance, and arrangement types of corrugated pipes: concave and convex, had a noticeable influence on hydrothermal behavior. The *Nu* was enhanced up 117% at low *Re,* and the friction factor was increased also up to 254% for all *Re* for heat exchanger made of convex inner corrugated pipe and concave outer corrugated pipe. Additionally, the maximum PEC achieved was about 1.2 for heat exchanger made of convex inner corrugated pipe and concave outer corrugated pipe.

Elshafei et al., [86] performed experiments on corrugated channels under turbulent flow conditions, as shown in Fig. 17. The results showed that heat transfer was significantly enhanced accompanied also by high-pressure drop. The average *Nu* and friction factor improved by 2.6–3.2 and 1.9–2.6 relatives to the smooth plate channel, respectively, according to the spacing and phase shift. It was observed that the friction factor increased when the channel spacing and corrugation phase shift increased. The hydraulic and thermal performance was greatly affected by the spacing variations more than the phase shift variation. They observed a great PEC could be obtained by using a corrugated plate channel,

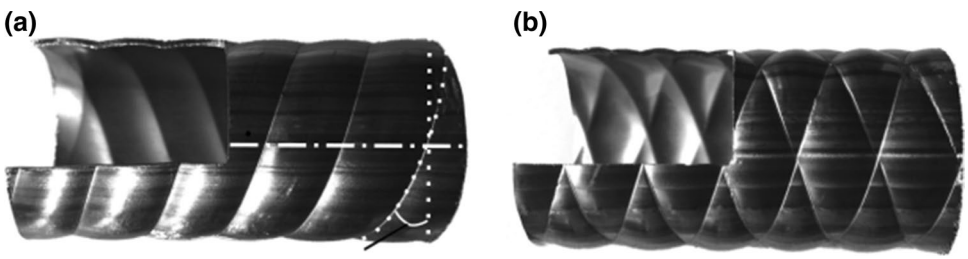

Fig. 15 **a** Single-structured and cross-structured tubes [84]

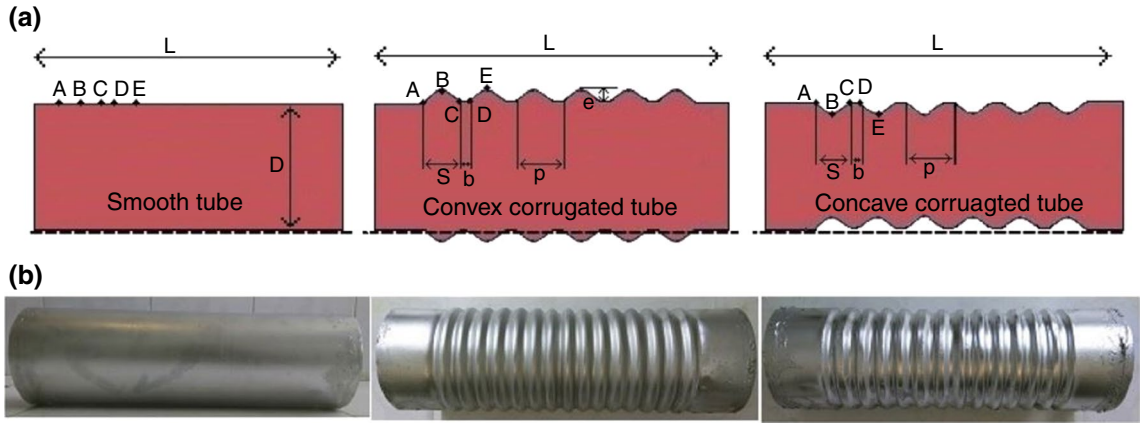

Fig. 16 **a** Scheme and **b** photograph of the corrugated tubes [85]

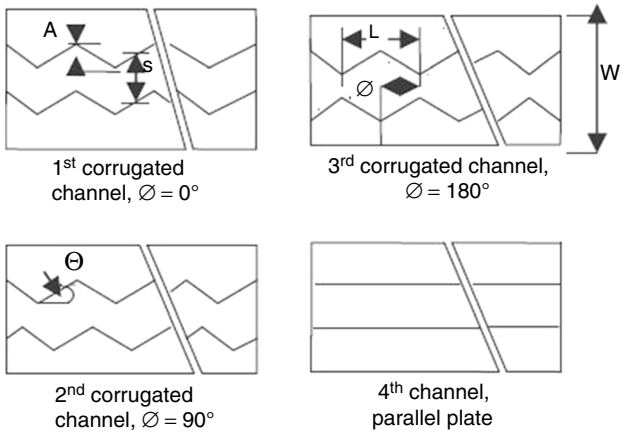

Fig. 17 Smooth and corrugated channel with different phase shifting [86]

and the maximum PEC was evaluated by optimizing the spacing and phase shift factors.

Bilen et al., [87] carried out experiments for developing the performance of a fully developed turbulent airflow in tubes without and with circular, trapezoidal, and rectangular grooves as shown in Fig. 18. The heat transfer was improved up to 63%, 58%, and 47% for the tube with circular, trapezoidal, and rectangular grooves, respectively, compared to the typical tube at $Re = 38{,}000$. The heat transfer rate of the tube with trapezoidal grooves was close to that with circular grooves, but it has a lesser groove number of 20%. On another hand, the flow disturbance in the pipe with trapezoidal grooves was greater than that with circular grooves because of the lower groove number. They reported an important notice that the pipe having grooves requires more cost because of groove machining. But for the corresponding

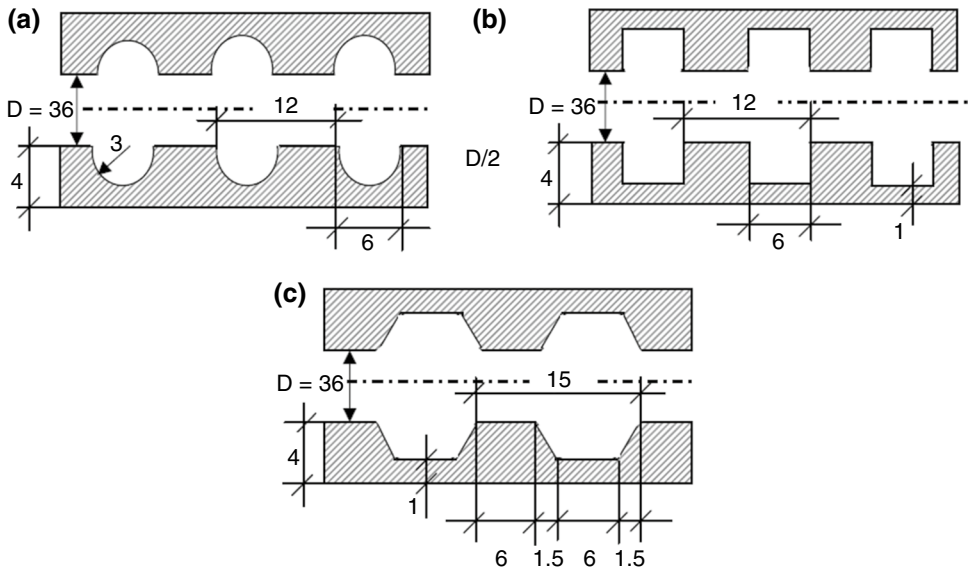

Fig. 18 Schematic diagram of the grooved tube, **a** circular, **b** rectangular, and **c** trapezoidal grooves [87]

thermal performance of the typical pipe, the heat exchanger will be shorter in length, lighter in mass, and smaller in size by grooving the pipes.

Han et al., [88] simulated computationally symmetric and asymmetric convex corrugated tubes using, as shown in Fig. 19, *k*-ε turbulent model. Both the *Nu* and pressure drop increased with increasing the corrugation depth. The PEC increased by increasing the radius of the circular corrugation. In general, it was found that the asymmetric corrugated tube revealed superior hydrothermal performance compared to the symmetric corrugated tube by about 8–18%.

Wang et al., [89] conducted a numerical investigation with some experiments to study the turbulent flow and heat transfer characteristics of outward transverse and helically corrugated tubes for turbulent flow conditions close to the case study of Han et al., [88]. It was published that the heat transfer was enhanced due to the turbulent fluctuation and boundary-layer redevelopment, whereas this enhancement was slightly affected by the rotational flow. However, the secondary flow and fluid pulsation were inhibited, and consequently, flow resistance was reduced. The maximum PEC value obtained was 1.40 at $Re = 3800$ at the corresponding geometric parameters detailed in their paper. They could obtain higher PEC for their proposed design compared to some designs such as the broken twisted tap in the smooth tube, the circular tube with wire coil insert, twisted oval tube, and internally finned tube. Consequently, the PEC declined sharply with increasing the *Re* number.

Du et al., [90] studied the effect of transverse sinusoidal ribbed tubes (SRTs) (corrugation toward the inner of the tube) numerically for laminar water flow in order to generate longitudinal vortex streams to intensify the flow mixing and to interrupt the thermal boundary layer as illustrated in Fig. 20. Their results inferred that *Nu* number and PEC increased when the rib height increased; the rib amplitude, rib width, and the rib pitch decreased. In addition, the *Nu* number and PEC increased when the circumferential rib numbers increased from 1 to 3 and then they decreased when the rib numbers ranged from 3 to 6. In general, the PEC was increased with the rise of *Re* number. The heat transfer was enhanced up to 4.89 times, and the friction loss was improved up to 5.62 times when the ribs were used. The maximum PEC recorded was about 3.64 using the sinusoidal rib technique.

Hong et al. [91] investigated the hydrothermal enhancement of wavy-corrugated tube over the range of $7500 < Re < 20{,}000$. Several parameters are examined, namely corrugation number, arrangement, corrugation width, corrugation height, corrugation amplitude. Water is employed as the working fluid. It was indicated that all wavy-corrugated tubes considered provided better hydrothermal performance than straight tube due to enhanced flow mixing induced by corrugations. In addition, the wavy-corrugated tube with the parallel arrangement is the best among other arrangements. The maximum PEC obtained is about 1.56 at *Re* of 7500 with a number of corrugation of 3, corrugation amplitude of 5 mm, corrugation width of 9 mm, and corrugation height of 1.4 mm.

Zhang and Che [92] studied numerically the hydrothermal performance of cross-corrugated (CC) plates; (sinusoidal, isosceles triangular, trapezoidal, rectangular, and elliptic corrugations) compact heat exchanger, as shown in Fig. 21, using the *k*-ε turbulence model. It was reported that the *Nu* and *f* were about 1–4 times higher for the trapezoidal channel

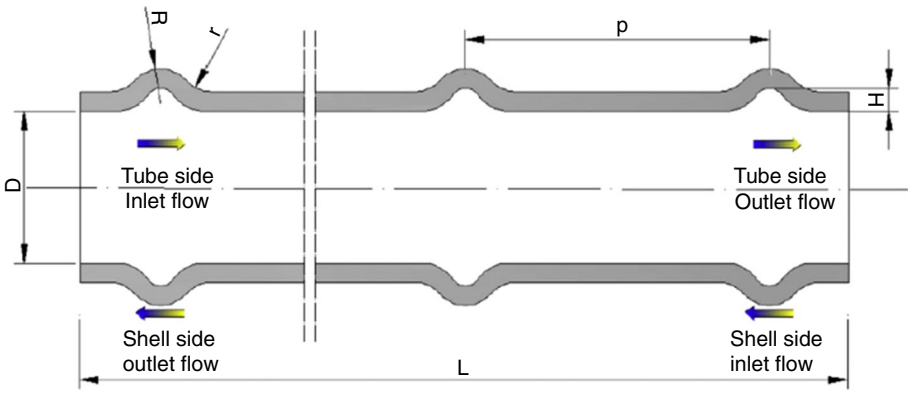

Fig. 19 Scheme of the convex-corrugated tube [88]

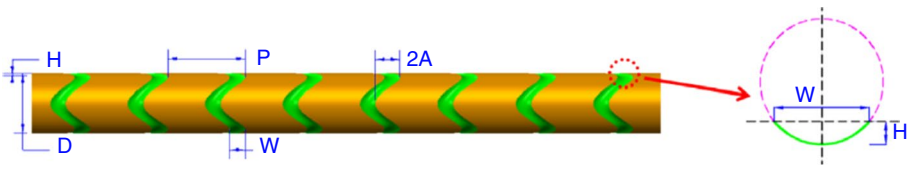

Fig. 20 Scheme of the sinusoidal-ribbed tube [90]

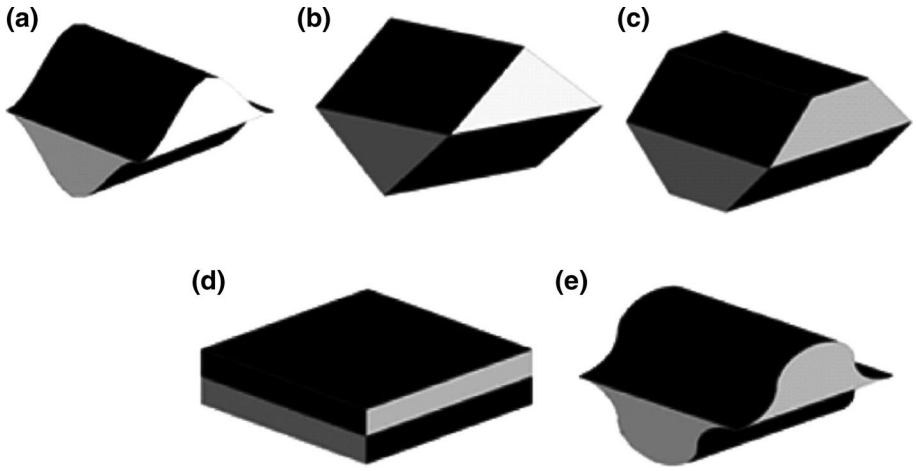

Fig. 21 Configurations of one cell of **a** sinusoidal, **b** triangular, **c** trapezoidal, **d** rectangular, and **e** elliptic corrugation [92]

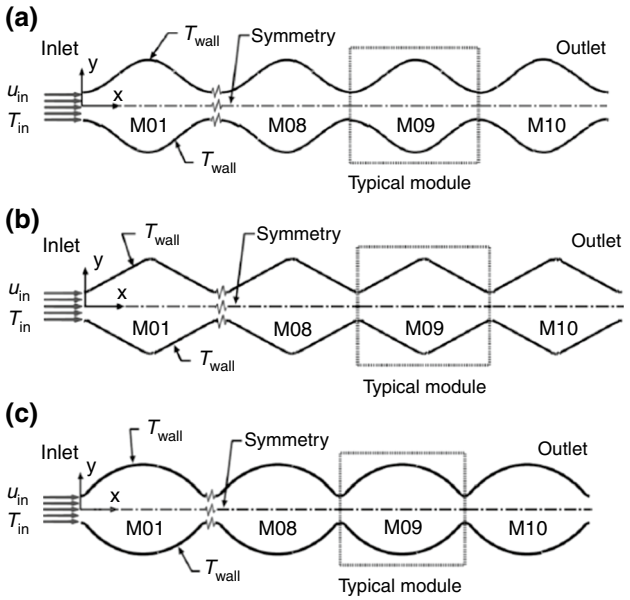

Fig. 22 Domain of the **a** sinusoidal-, **b** rounded-vee-, and **c** rounded-elliptic-corrugated plate [93]

than for the elliptic channel. Higher *Nu* and friction factor were observed with the trapezoidal cross-corrugated plate compared with others, whereas the elliptic CC plate had the inferiority in terms of heat transfer and friction losses. Moreover, it was seen that the elliptic and sinusoidal CC plate exhibited the highest PEC relative to others.

Ferley and Ormiston [93] studied a steady 2D laminar forced convection in sinusoidal-, rounded-elliptic-, and rounded-vee-corrugated plate as schematically demonstrated in Fig. 22. It was revealed that the sinusoidal corrugation demonstrated the lowest friction factor and highest average *Nu* number among other shapes. Moreover, the rounded-elliptic-corrugated shape showed the greatest heat transfer per unit pumping power at $Re = 300$ and provided a larger recirculation region relative to other patterns. In general, increasing the cavity depth of the corrugation could increase the number of recirculation zones. In addition, the hydraulic performance of the sinusoidal- and rounded-vee-corrugated shapes was identical approximately.

Bahaidarah et al. [94], studied also a 2D laminar fluid flow and heat transfer in a periodic sinusoidal- and arc-wavy channel for $Pr = 0.7$. At low flow rates, two configurations illustrated a little or no heat transfer enhancement compared to the parallel-plate passage. The heat transfer was enhanced up to 80% in some cases of the sinusoidal pattern at higher *Re* numbers. The recirculation size and strength were decreased when the height ratio or the length ratio increased for both configurations. The arc-wavy channel showed a higher pressure drop compared to the sinusoidal pattern. The average *Nu* raised monotonically with increasing *Re*. The *Nu* number ratio was less than unity for most cases, so they recommended that such channels can be used in applications in which pumping power is not in short supply.

Multiple techniques

Corrugation with perforations

Caliskan [9] examined experimentally two heat transfer enhancement techniques: impingement of circular air-jet and transverse rib surfaces with/without perforations to show their effect on the heat transfer and flow characteristics of a rectangular channel. They monitored a thermal superiority when the perforated rib surfaces were used compared to the channel having solid ribs (without perforations). The turbulence kinetic energy and radial velocities were greater for the perforated transverse ribs as compared to the using of solid ribs. The maximum average *Nu* enhancement observed was 48% over the smooth surface depending on the rib shape,

jet-to-plate distance, and the flow rate value. They derived correlations for the average *Nu* when the perforated ribs were implemented within ± 12% deviation with the experimental data.

Hassan et al. [95] experimentally studied the effect of using v-corrugated-perforated absorber, as shown in Fig. 23, on the performance of flat-plate double-pass solar air heater. Several air mass flow rates are tested with two absorber plates: corrugated and corrugated-perforated plates. Corrugated-perforated plate exhibited the highest daily efficiency of 71.85%. Zheng et al., [6] developed the design of the glazed transpired solar collector by using a perforating corrugated plate mathematically and experimentally. They highlighted that their proposed design would be applicable enough due to its advantages in terms of economy and thermal performance in village cold zones. The thermal efficiency of the new design decreased with increasing the inlet temperature, collector width, and porosity, while it increased with increasing the ambient air temperature, radiation intensity, and collector height. The augmentation of thermal efficiency reduced with increasing the flow rate, radiation intensity, and collector height. Their predicted mathematical results of the thermal performance for the proposed model was deviated 3.6% from the experimental data.

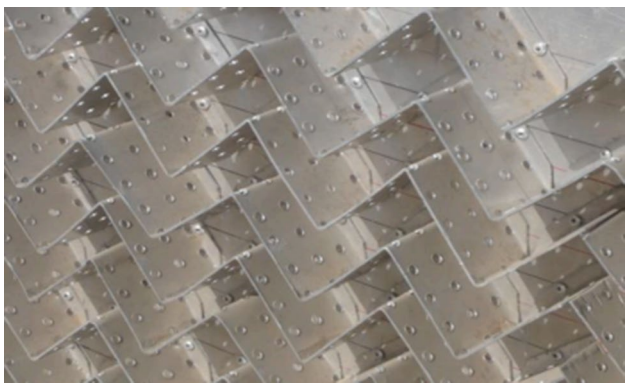

Fig. 23 Corrugated-perforated absorber [95]

Zhang et al. [96] developed mathematically the thermal design of a solar air collector by using a slit-perforated corrugated plate (wavy plate with inclined waves) for enlarging the heat collection area and increasing the jet impingement more. It was reported that the height of the absorber plate has the largest effect on the thermal performance among structure parameters. When the air velocity in the collector increased up to 1.14 m s^{-1}, the efficiency increased became 67.83%. Among the transpired solar air collectors, their suggested design provided higher thermal performance. Their proposed design could produce 820.7 MJ in the hot season to save 43.1 kg of standard coal and consequently reduce 102.1 kg of carbon dioxide emission. They verified the results of the outcome with the experimental data within an average deviation of 4.8%. The details of their proposed design are illustrated schematically in their paper.

Aliabadi et al. [10] modified experimentally the thermal design of wavy perforating plate–fins heat exchangers for reducing their size as shown in Fig. 24. They investigated the effect of three passive techniques for heat transfer enhancement: perforations, winglets, and nanofluids (0.1 and 0.3 vol.%), and *Re* number is ranged from 3900 to 11,400 on heat transfer and flow specifications under turbulent flow regime. It was displayed that the winged wavy plate–fins technique outperformed the others in terms of heat removal, followed by the perforated one, and then the nanofluid. Moreover, they showed the same trend of the increase in frictional losses. The perforated wavy plate–fins displayed the same heat transfer and friction factor with the nanofluid when *Re* number was over 7000. The hydrothermal performance was greater than unity for all three techniques used. Its highest value was for the winged wavy plate–fins (around 1.26) compared to the typical one at the lowest *Re* number value and the highest waviness aspect ratio. They recommended using the winged wavy plate–fins in the heat exchangers as an effective interrupted surface. In addition,

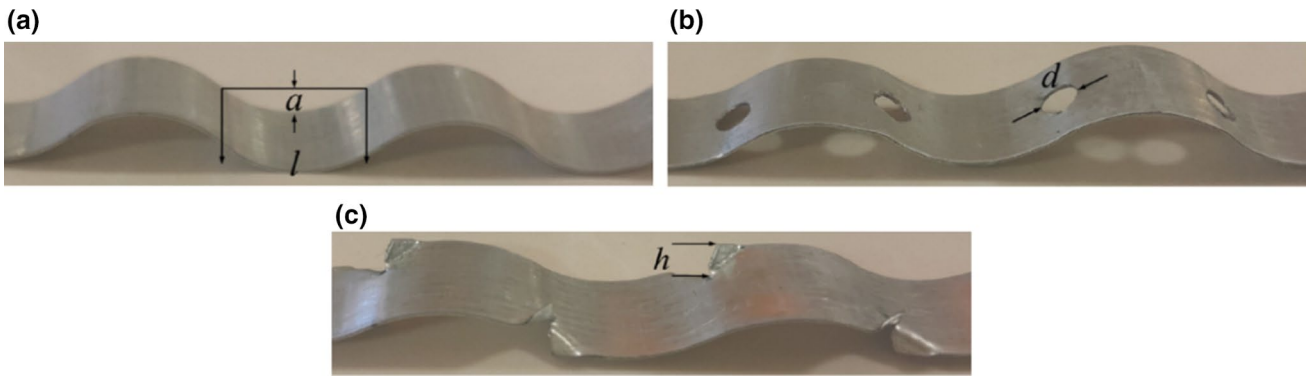

Fig. 24 Photograph of **a** typical wavy plate–fin, **b** perforated wavy plate–fin, and **c** winged wavy plate–fin [10]

Aliabadi et al. [97] improved the efficiency of the hydrothermal performance of corrugated-perforated fin (CPF) in a solar heating system. Water and Al_2O_3–water nanofluid were used as coolants. The wave aspect ratio, perforation diameter, nanoparticle concentration, and flow rate were evaluated. Their experimental results demonstrated that the heat transfer rate of the modified design was greater than that of a typical pattern, whereas the pressure drop was lower. The maximum hydrothermal performance was 1.95 at $Re \approx 7000$, the waviness aspect ratio of 0.51, perforation diameter of 6 mm, and flow rate of 0.117×10^{-3} m^3 s^{-1}. The greatest increase in the heat transfer coefficient and pressure drop was 14.1% and 9.5%, respectively, at 0.3 vol.%.

Corrugation with PCM

Ameri et al. [98] conducted an experimental investigation of v-corrugated solar air heater with the implementation of PCM using paraffin packs, as indicated in Fig. 25. Two kinds of paraffin wax with different melting temperatures along with four PCMs arrangements are tested. Utilizing PCM enhanced the daily thermal efficiency from 53.1% to 62.6%. Also, outlet temperature increased by 5 C^o due to using PCM with high melting temperature, and equally distributed PCM exhibited the optimal daily performance. Kabeel et al. [99] carried out experiments on flat and v-corrugated plate solar air heaters with built-in phase change material (PCM) as a thermal energy storage material under the weather condition of Tanta city—Egypt. It was monitored that the outlet temperature of the corrugated plate model could raise from 1.5 to 7.2 °C greater than the ambient temperature during 3.5 h after sunset when the PCM was used in comparison with 1–5.5 °C during 2.5 h after sunset for the flat pattern at an airflow rate of 0.062 kg s^{-1}. The daily efficiency of the corrugated plate pattern with PCM was 12% more than the corresponding values without PCM, and it was also 15% and 21.3% greater than the corresponding ones for the flat plate with and without PCM, respectively, at the same above flow rate value. By increasing the mass flow rate, the daily and instantaneous thermal efficiency would be increased regardless of the use of PCM. In contrast, the air temperature difference across the heater, the amount of heat stored, and the PCM freezing time were decreased. In general, the heat transfer rate of the v-corrugated sample was much larger than that of the flat one despite the use of PCM and it increased with increasing the air mass flow. They also studied the effect of the PCM thickness on the temperature difference across the heater as the reader could go through their paper thoroughly. They recommended using the PCM due to its efficient effectiveness in improving the thermal performance of the v-corrugated plate solar air heater.

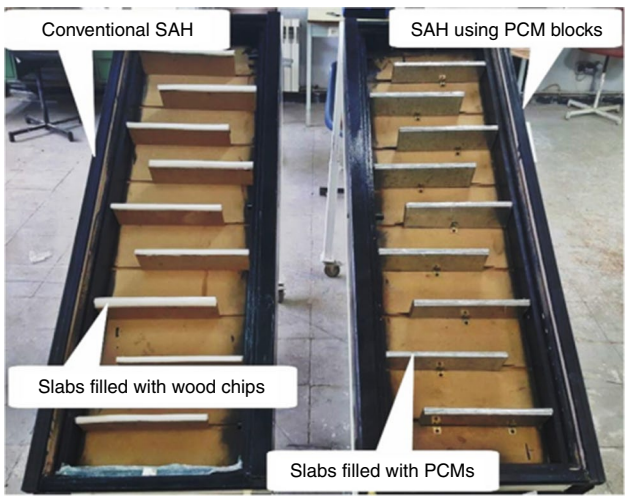

Fig. 25 Illustrative scheme of semicircle-corrugated channel [98]

Corrugation with nanofluids

Aliabadi [100] performed a computational study on using Al_2O_3–water nanofluid (0–4 vol.%) as a coolant in a sinusoidal-corrugated channel to show its effect on the heat transfer and flow characteristics. Besides, he studied the effect of the height and length of the channel, wavelength, wave amplitude, and phase shift for $6000 < Re < 22{,}000$. It was inferred that the channel height and wave amplitude influenced significantly the *Nu* and friction factor. The nanofluid offered greater heat transfer rates in comparison with the base fluid, while a slight increase in the friction factor was observed. The highest PEC obtained was ~ 2.4 at 4 vol.%, and the largest wave amplitude and wavelength examined. He correlated based on the nanofluid used for predicting the *Nu* and friction factor through sinusoidal-corrugated channels.

Also, Aliabadi and his research group [3] evaluated the hydrothermal performances of a plate and plate–pin-corrugated mini-CHS having triangular, trapezoidal, and sinusoidal shapes for laminar flow regime. Water and Al_2O_3–water nanofluid were used as cooling fluids. Their numerical and experimental results displayed that the corrugated plate–fins HS could enhance the heat transfer rate with a moderate increase in the pressure drop penalty compared to the straight pattern. The highest increase in the heat transfer and pressure drop was recorded with the trapezoidal corrugation channel. The heat transfer coefficient was increased, and the pressure drop was decreased by about 22.9% and 49.3%, respectively, when the pins were used in the sinusoidal corrugation configuration in comparison with no pins pattern. In general, the nanofluid could augment the heat transfer with a moderate increase in the pressure drop. They highlighted that the hydrothermal performance of some cases was less than unity and others were greater depending on the corrugation shape and the value of *Re* number.

The maximum hydrothermal performance factor was 1.84 when nanofluid (0.3 vol.%) was used instead of water in the sinusoidal plate–pin fins. They stated that designers can reduce the pumping power in the corrugated HS for the same heat dissipation. In addition, we believe that the designers can reduce the heat sink size, while the heat transfer rate remains constant. Wang et al. [101], experimentally tested the influence of using TiO2-H_2O nanofluids as a working fluid on the hydrothermal performance of corrugated tubes. Different corrugation pitches are tested as well. Using the mass fraction of the nanofluid of 0.5%, heat transfer was improved by 36.3% for different corrugation pitches. Also, it is revealed that the maximum hydrothermal performance achieved in the study is 1.56.

Ajeel et al., [102] optimized the height/width ratio and pitch/length ratio of the symmetry semicircle-corrugated channel with SiO_2–water nanofluid (0–8.0 vol.%) numerically for $10{,}000 < Re < 30{,}000$ in order to make it more compact. It was revealed that the height/width ratio showed a greater heat transfer rate compared to the pitch/length ratio. At the highest value of *Re*, *Nu* number was increased up to 13.59% when the pitch/length ratio decreased from 0.175 to 0.075, whereas it increased by about 78.84% when the height/width ratio increased from 0.0 to 0.05. The optimal hydrothermal performance was found to be 2.95 at the height/width ratio of 0.05, the pitch/length ratio of 0.075, and the volume fraction of 0.08 when *Re* number was at its lowest value. This enhancement was reduced by increasing the flow rate. Moreover, they derived correlations for *Nu* and friction factor using nanofluids in a corrugated channel according to their study conditions. See Fig. 26.

Ahmed et al., [103], Ahmed et al. [104], and Ahmed et al. [105] published a computational study on the heat transfer and Cu– and CuO–water nanofluid (0–5 vol.%) flow characteristics in sinusoidal-, triangular-, and trapezoidal-corrugated channels under the laminar flow regime. It was stated that the heat transfer and pressure drop were improved by increasing the nanoparticle concentration and *Re*. In addition, they did not report a significant addition to the pressure drop penalty. The friction coefficient and *Nu* would be increased by increasing the amplitude of the wavy channel. The PEC was increased by increasing the flow rate. In general, the trapezoidal channel provided the greatest *Nu* number followed by the sinusoidal, triangular, and then straight channel. They also showed in their research [103] that the average *Nu* was augmented with the increase in the volume fraction and the amplitude of the corrugated channel. Besides, this enhancement was accompanied by an increase in the pressure drop. It was also found that the *Nu* number increased and the pressure drop decreased when the wavelength of the corrugated channel decreased. The highest heat transfer improvement registered was 43.9% at $Re = 200$, whereas the maximum PEC was about 1.46 at the highest *Re* number and 5 vol.%.

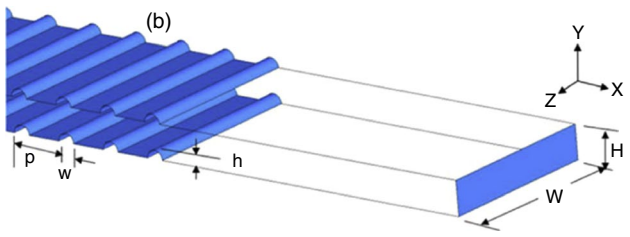

Fig. 26 Illustrative scheme of semicircle-corrugated channel [102]

Also, Ahmed and his group [4] studied numerically the effect of the shifting of the sinusoidal-wavy surface on the laminar forced convection flow using Al_2O_3–water nanofluid. The sinusoidal-wavy channel with different phase shifts, namely 0°, 45°, 90°, and 180°, was investigated. It was indicated that the optimal PEC obtained was 1.46 at 0° phase shift channel (where the cross-sectional area of the wavy channel remains constant along the flow direction) at high laminar *Re* number and 5vol.% nanofluid.

Ahmed et al. [106] cooled straight-, trapezoidal-, and sinusoidal-corrugated channels by using SiO_2–water nanofluid (0–1 vol.%) for $100 < Re < 4000$ numerically and experimentally. The thermophysical properties of the nanofluid were empirically measured. They confirmed that the *Nu* and *f* increased with the volume fraction. The trapezoidal-corrugated channel outperformed the others in terms of heat transfer, whereas the sinusoidal-corrugated channel was the second better one in comparison with the straight pattern.

Qi et al., [5] used TiO_2–water nanofluids as a working fluid in a stainless-steel-corrugated tube and a circular tube numerically and validated their data with their experiments. They reported that adding nanoparticles into deionized water did not show a significant additional resistance loss. A remarkable heat transfer enhancement was observed when both techniques were used simultaneously: corrugated tube and nanofluid, which enhanced the heat transfer by about 54%.

Goodarzi et al., [107] investigated computationally and experimentally the thermophysical properties of Gum Arabic-treated multi-walled carbon nanotubes (MWCNT-GA), functionalized MWCNT with cysteine (FMWCNT-Cys) and silver (FMWCNT-Ag) which were used as coolants. The effect of these coolants on the hydrothermal performance of the counterflow corrugated plate heat exchanger was studied under the turbulent flow regime and (0–1 vol.%). They measured the nanofluid properties experimentally. It was found that increasing *Re* number, Peclet number, and/or volume fraction would improve the heat transfer rates of the nanofluid. A rise in the pumping power was recorded when *Re* number and/or volume fraction increased, whereas this penalty was relatively insignificant. The heat removal

was greater for nanofluids in comparison with water for the corresponding pumping power.

Naphon and Wiriyasart [108] combined both passive and active heat transfer enhancement techniques, namely (TiO_2 nanofluids and helically corrugated rib) and (pulsating flow and magnetic field) to show their effect on the thermal and hydraulic performance through a circular tube. Nanofluid with a concentration of 0.25%, and 0.5%, pulsating flow frequency of 10, 15, 20 Hz, and helical-corrugated rib with the depth and pitch of 1.25 mm, 6.35 mm, respectively, were involved in their experimental investigation. The comparison with the smooth tube showed that the nanofluid improved significantly the heat transfer rate. The disturbing of nanoparticles Brownian motion by the magnetic field and pulsating flow frequency exhibited a great heat transfer enhancement. The disturbance of nanoparticles suspended in water was induced by the centrifugal force, magnetic force, and roughness of the helically corrugated ribs in which a higher heat transfer rate was recorded with a slight increase in the frictional forces was registered. Therefore, their results would allow investigators to design cooling systems with higher thermal performance for cooling electronic chips.

Mei et al., [109] carried out experiments in order to investigate the hydrothermal performance of Fe_3O_4–water nanofluid in a corrugated tube under a magnetic field. The ranges of the magnetic induction intensities were 0–300 G, nanoparticle mass fractions were 0–0.5%, electromagnet arrangement modes were one-side electromagnet and two-side staggered electromagnet, a smooth and corrugated tube, and *Re* numbers were 800–12,000. It was shown that the heat transfer enhancement was influenced by the nanoparticle concentration, magnetic induction intensity, two-side staggered electromagnet, and corrugated tube. The *Nu* was improved up to 10.0% and 17.6% when the nanofluid flow through the smooth and corrugated tube, respectively, under the magnetic field in comparison with water. The *Nu* of nanofluids with two-side staggered electromagnets would be improved by 2.0% compared to the one-side electromagnets. They displayed that the PEC would be increased with the increase in *Re* at first and then decrease. They concluded that coupling these passive and active techniques could augment the heat transfer noticeably with a slight increase in the flow resistance.

Conclusion and remarks

The recent and advanced developments of compact heat exchangers surface using corrugations (as a passive heat transfer enhancement techniques) alone or combined with other methods (passive, active, or passive and active together) for enhancing the hydrothermal performance have been discussed and analyzed in this paper. Experimental and numerical investigations covering conduits with corrugation in different shapes such as helical, transverse, wavy, zigzag, converging–diverging, and others are covered. Also, these corrugations are applied in several types of heat exchangers passages such as tubes, heat sinks, and solar collectors. It can be concluded as:

- This review of the literature shows that the *Nu* and friction factor were increased with increasing the height, and width of helical and transverse corrugation, and decreasing the pitch ratio. The angle of helical corrugation was optimized between 20° and 30°. However, the PEC was greater than unity. Some researchers claimed that the increase in the friction factor was greater than the increase in the *Nu*.
- A high heat transfer rate was noticed with an increase in the wave amplitude of wavy and converging–diverging corrugated channel, but it was accompanied by an increase in the friction factor as some authors proved that. In zigzag-corrugated channels, the thermal performance was augmented as the wave angle increased. In addition, the increase in the channel height could lead to an increase in the Nu as well as the friction factor.
- Researchers have found that the wave amplitude of corrugations applied in MCHS and mini-CHS has a larger impact on heat transfer and pressure drop compared to the wavelength. Employing secondary branches in wavy MCHS could improve the thermal performance compared with classical wavy MCHS. Moreover, corrugating the surface of solar air collectors would enhance the thermal efficiency by about 5–20% in comparison with the flat model.
- Cross-corrugated surfaces showed higher thermal performance than v-corrugated surfaces, and also elliptical and sinusoidal CC exhibited high PEC compared to other shapes as most of the researchers claimed. Some researches revealed that circular grooves in tubes displayed high augmentation in *Nu* compared to trapezoidal and rectangular grooves. Furthermore, the transverse-corrugated tubes outperformed that corrugated helically in terms of heat transfer rate.
- The heat transfer rate was enhanced, and the pressure drop was reduced when perforated corrugated surfaces were implemented. Using the PCM in corrugated plates was recommended with daily efficiency of 21.3% higher than that without PCM. In addition, increasing heat transfer rate was monitored using nanofluids but that was accompanied with an increase in the pressure drop.

In brief, the above survey of the available literature can be summarized in such a table as the main variable parameters of the corrugated channel are illustrated with the concrete findings resulted from this technique as shown in Table 1.

Table 1 Summary of corrugation enhancement technique

Category	Reference	Variable parameters	Results obtained
Circular-corrugated channel (helical corrugation)	Harleß et al., [11]	Angle, height, and pitch of single-start and three-start corrugations	Single-start-corrugated tube exhibited the highest thermal performance
	Wang et al. [12],	Circular-, square-, and triangle-corrugated tubes with different tube spacings	Triangular-corrugated tube showed the highest hydrothermal performance
	Laohalertdecha and Wongwises [13]	Different pitches and depths of copper-corrugated tubes	Nu increases with increasing corrugation pitch and depth
	Vicente et al. [14],	The severity index	corrugated tube with intermediate severity gives the best choice
	Harleß et al. [15],	Corrugation pitch and angle	Optimum angle of 38.4°gives the highest thermal performance
	Rozzi et al. [16],	Effect of corrugated tubes on fluid flow in Newtonian and non-Newtonian	Moderate heat transfer improvement was obtained but with high-pressure drop
	Wang et al., [17]	Corrugation height-to-diameter and pitch-to-diameter ratios	Height-to-diameter and pitch-to-diameter ratios should be less than 0.1 and 2 for enhancing hydrothermal performance
	Córcoles et al. [18],	Corrugation height-to-diameter ratio	*Nu* and pressure drop were improved as the height-to-diameter increased
	Xin et al. [19],	Two-start helically corrugated tube, oscillatory flow	The highest PEC is 1.69
	Dong et al. [20],	Spirally corrugated tubes, water and oil	High Nu and pressure drop compared to smooth tube
	Pethkool et al. [21],	Pitch-to-diameter ratio and rib height-to-diameter ratio	The maximum PEC was 2.3 with a pitch ratio of 0.27 and a rip height ratio of 0.06
Circular-corrugated channel (transverse corrugation)	Xiao-Wei et al. [22],	Corrugation height	Heat transfer and fluid flow increased as the roughness height exceeded the viscous sublayer thickness
	Jaffal et al. [23],	Interruptions to the perimeter of the corrugations	The maximum performance factor achieved is 1.28
	Sun and Zeng [25]	Transversely corrugated tubes	Heat transfer and pressure drop are both increased
	Mohammed et al. [26],	Rib pitch-to-diameter, rib width-to-diameter, and rib height-to-diameter	Best overall enhancement is 30% at rib height-to-diameter of 0.025
	Huang et al. [28],	Rib height	Thermal performance in falling film evaporation is higher compared to smooth tube

Table 1 (continued)

Category	Reference	Variable parameters	Results obtained
Non-circular-corrugated channel (wavy corrugation)	Piroozfam et al. [29],	Frequency of the sinusoidal-wavy plate	PEC was reduced with increasing wavy plate frequency
	Mirzaei et al. [30],	Wave amplitude of half-wavy-corrugated channel	The optimal thermal performance parameter was 1.19 at a wave amplitude of 0.1
	Zhang et al. [31],	Wave amplitudes of curved wavy-corrugated channel	Maximum thermal performance is achieved with a combination of wavelength and wave amplitude
	Tsai et al. [32],	Two wavy cross-corrugated channels	Experimental data are 20% higher than simulated results
	Ma et al. [34],	Offset-bubble primary surface channel, wavelength, and wave height	Wavelength showed higher effect on thermal performance compared to wave height
	Hasis et al. [35],	Twisted sinusoidal-wavy microchannel, aspect ratio, the waviness, and extent of twist	Nu augmented with increasing channel waviness and aspect ratio. The maximum goodness factor achieved was 1.35
Non-circular-corrugated channel (zigzag corrugation)	Naphon [36]	Tilt angles	increasing tilt angle augmented heat transfer rate
	Naphon and Kornkumjayrit [37]	Tilt angle and channel height	the wavy angle of 40° provided the best thermal performance
	Luo et al. [38],	Wavy fins and vortex generators	Maximum PEC was 1.23
	Mohammed et al. [40],	Corrugation tilt angle, channel height, and wave height	the wavy angle of 20° provided the best thermal performance
Non-circular-corrugated channel (converging–diverging corrugation)	Parlak et al. [41],	Channel width, wavelength, and amplitude	Maximum PEC was 1.7
	Wang and Chen [43]	Amplitude–wavelength ratio	The larger the amplitude–wavelength ratio the higher the heat transfer rate
	Pehlivan [44]	Rounded and sharp corrugation peaks, different corrugation angles, pitches, and heights	The maximum heat transfer enhancement was about 15 times larger than the straight channel
Corrugated heat sink (microscale)	Gong et al. [46],	Wave amplitude, wavelength, and aspect ratio	The maximum PEC was 1.55
	Pourhammati and Hossainpour [47]	Wave amplitude and wavelength	The maximum PEC was 1.338
	Mohammed et al. [49],	Dimensionless wave amplitudes	Dimensionless wave amplitudes of 0.21875 lead to optimum thermal performance
	Yong and Teo [51]	Aspect ratio and amplitude ratio	The maximum achieved PEC was 1.6
	Sui et al. [53],	Wave amplitude	Maximum heat transfer enhancement was 211%
	Chiam et al. [56],	Waviness amplitudes	The maximum PEC was 1.9

Table 1 (continued)

Category	Reference	Variable parameters	Results obtained
Corrugated heat sink (mini-scale)	Khoshvaght-Aliabadi et al. [57],	Changing the cross section size of the routes	Divergent model is the best in terms of hydrothermal performance
	Aliabadi and Nozan [58]	Triangular, sinusoidal, and trapezoidal corrugated mini-channel heat sink	The highest performance factor was achieved with a sinusoidal pattern
	Aliabadi and Sahamiyan [59]	Wavelength, wave amplitude, nanoparticles concentration	The maximum PEC obtained was 3.5
	Aliabadi et al. [60],	Integral and interrupted pin–fins	The highest obtained performance factor was 2.65
	Khalifa and Jaffal [62]	Wavy and helical corrugations. Aspect ratio, pitch ratio, wave amplitude ratio, and solid void fraction	Highest PEC obtained was 1.16 for helical corrugation
Corrugated solar collector	Abdullah et al. [63],	Flat trays solar still, corrugated trays solar still, and conventional solar still. phase change material (PCM) mixed with CuO nanoparticles	Total freshwater yield of corrugated trays solar still was increased by 122%
	Younes et al. [64],	Flat, corrugated, half barrel, and conventional solar stills	Daily productivity for corrugated solar still is improved by 134%
	Aboghrara et al. [65],	Circular jet impingement	The optimal thermal efficiency was 14% higher than the smooth duct
	Dormohammadi et al. [67],	Richardson number, wave amplitude and wavelength, and nanoparticles concentration	The total entropy generation increased with reducing Richardson number and increasing nanoparticles concentration
	Kumar and Chand [69]	Herringbone-corrugated fins	The thermal efficiency was improved by around 20%
	Zhang et al. [74],	Air, water, and air–water compound heating in flat-plate solar collector with dual-function	Thermal efficiency of air–water compound mode of 73.4% was the highest among others
	El-Sebaii et al. [8],	Double-pass flat and v-corrugated plate solar air heaters	Thermal efficiency of 14% higher than the flat mode
	Hedayatizadeh et al., [77]	Double-pass/glazed v-corrugated plate solar air heater	Maximum exergy efficiency of the proposed collector was 6.27%
	Karim and Hawlader [78]	Flat-plate, finned, and v-corrugated solar air collectors	The v-corrugated heater was the most efficient mode
	Farhan et al., [79]	Effect of channel numbers and twisted ratio	Thermal efficiency was enhanced by 17.5%

Table 1 (continued)

Category	Reference	Variable parameters	Results obtained
Configuration of corrugation	Liu et al., [80]	Cross-corrugated and v-corrugated solar air collectors	The highest thermal efficiency was 78% implementing cross-corrugated solar collector
	Akbarzadeh et al., [81]	Sinusoidal- and triangular-corrugated plates. Influence of using Cu–water as the working fluid	Maximum thermal performance was enhanced by 72.4%
	Rainieri and Pagliarini [82]	Helical and transverse corrugated tubes	Helical corrugation is preferable
	Nelly et al. [84]	Helically single-structured and cross-structured tubes	The hydrothermal performance of cross-structured tubes was the highest
	Dizaji et al. [85]	Inner and outer corrugated tubes of double-pipe heat exchanger	Maximum PEC achieved was about 1.2 for heat exchanger made of convex inner corrugated pipe and concave outer corrugated pipe
	Bilen et al., [87]	Tubes with circular, trapezoidal, and rectangular grooves	Heat transfer rate was improved by 63% for circular grooves
	Han et al., [88]	Symmetric and asymmetric convex corrugated tubes	Asymmetric corrugated tube revealed superior hydrothermal performance
	Du et al., [90]	Transverse sinusoidal ribbed tubes. Rib height, rib amplitude, rib width, rib pitch	Maximum PEC recorded was about 3.64
	Hong et al. [91]	Corrugation number, arrangement, corrugation width, corrugation height, corrugation amplitude of wavy tubes	The maximum PEC obtained was about 1.56
	Zhang and Che [92]	Sinusoidal, isosceles triangular, trapezoidal, rectangular, and elliptic corrugations compact heat exchanger	Elliptic- and sinusoidal-corrugated plate exhibited the highest PEC relative to others
	Ferley and Ormiston [93]	Sinusoidal-, rounded-elliptic-, and rounded-vee-corrugated plate	Sinusoidal corrugation demonstrated the lowest friction factor and highest average *Nu* number among other shapes
Multiple techniques (corrugation with perforations)	Caliskan [9]	Impingement of circular air-jet and transverse rib surfaces with/without perforations	The maximum average *Nu* enhancement observed was 48%
	Hassan et al. [95],	Corrugated and corrugated-perforated flat-plate double-pass solar air heater	The highest daily efficiency was 71.85% using corrugated-perforated plate
	Zhang et al. [96],	Slit-perforated corrugated plate	Effective efficiency reached the peak of 67.83%
	Aliabadi et al. [10],	perforations, winglets, and nanofluids	Winged wavy plate–fins technique outperformed the others in terms of heat removal, followed by the perforated one, and then the nanofluid
	Aliabadi et al. [97],	Corrugated-perforated fin in a solar heating system. wave aspect ratio, perforation diameter, nanoparticle concentration,	The maximum hydrothermal performance was 1.95

Table 1 (continued)

Category	Reference	Variable parameters	Results obtained
Multiple techniques (corrugation with PCM)	Ameri et al., [98]	V-corrugated solar air heater with the implementation of PCM using paraffin packs, two kinds of paraffin wax	Utilizing PCM enhanced the daily thermal efficiency from 53.1% to 62.6%
	Kabeel et al. [99],	V-corrugated plate solar air heaters with built-in phase change material (PCM)	It was recommended to use the PCM due to its efficient effectiveness in improving the thermal performance
Multiple techniques (corrugation with nanofluids)	Aliabadi [100]	Sinusoidal-corrugated channel, Al_2O_3–water nanofluid, height and length of the channel, wavelength, wave amplitude	The highest PEC obtained was 2.4 at 4 vol.% with the largest wave amplitude and wavelength
	Ahmed et al. [4],	Effect of the shifting of sinusoidal-wavy surface, Al_2O_3–water nanofluid	The optimal PEC obtained was 1.46 at 5vol.% nanofluid
	Ahmed et al. [105],	Sinusoidal-, triangular- and trapezoidal-corrugated channels, Cu– and CuO–water nanofluid	The trapezoidal channel provided the greatest *Nu* with increasing nanoparticle concentration
	Ahmed et al. [106],	Trapezoidal- and sinusoidal-corrugated channels using SiO_2–water nanofluid	Trapezoidal-corrugated channel outperformed the others in terms of heat transfer
	Qi et al., [5]	TiO_2–water nanofluids, stainless-steel-corrugated tube and a circular tube	Corrugation and nanofluid enhanced the heat transfer about 54%
	Mei et al., [109]	Fe_3O_4–water nanofluid in a corrugated tube under a magnetic field	The *Nu* was improved up to 17.6% when the nanofluid flows through corrugated tube

Outlook for future works

Many efforts are required to be spent on thermal performance enhancement using the technique of surface corrugating. These days, researchers' attention is necessary to be focused on multi or compound heat transfer enhancement techniques for getting much higher heat dissipation with acceptable increase in the pumping power. From the above survey, it seems that there are some research topics that need to be fulfilled.

It can be said that no research is available on using non-uniform wavy- or zigzag-corrugated channel (i.e., reducing the wavelength as required, at the entrance flow region, for example, and increasing the wavelength when it is unnecessary, it at the fully developed region, for example). Providing new designs of corrugated channels offers high heat transfer keeping the solid volume constant. Optimizing the shape and number of the corrugation on the heat transfer and the pressure drop may be studied. Combined vortex generators with corrugated tape insertion are not studied yet. There is no study published on using corrugation technique with porous media with different porosities, PPIs, and porous properties uniformity. Due to the quick progress in the nanotechnology, same thermal performance can be obtained by corrugating the traditional heat exchanger, while the overall size is minimized. There is lack of publication in applying the corrugation technique in annulus heat exchangers. It is necessary to investigate the effect of oscillating flow (unsteady-state flow) in a corrugated channel. We apply a magnetic field on the nanofluid inside a corrugated enclosure to show the interaction between the metallic-nanoparticle movement and the corrugated walls. In addition, how can the helical-corrugated tubes keep the stability of nanofluids and reduce the sedimentation occurs due to the agglomeration.

From the point of view of the authors, the above suggested research areas are still hot topics and need more attention from investigators to optimize the hydrothermal performance of corrugated channels experimentally, numerically, and/or theoretically. This great challenge encourages the researchers to obtain efficient thermal system design of heat exchangers, lower power consumption, and saving the environment better than the existence.

References

1. Balla HH. Enhancement of heat transfer in six-start spirally corrugated tubes. Case Stud Therm Eng. 2017;9:79–89.
2. Barba A, Rainieri S, Spiga M. Heat Transfer Enhancement in a Corrugated Tube. Int Commun Heat Mass Transfer. 2002;29:3013–322.
3. Aliabadi MKh, Hassani SM, Mazloumi SH. Comparison of hydrothermal performance between plate fins and plate-pin fins subject to nanofluid-cooled corrugated miniature heat sinks. Microelectron Reliab. 2017;70:84–96.
4. Ahmed MA, Yusoff MZ, Ng KC, Shuaib NH. The effects of wavy-wall phase shift on thermal-hydraulic performance of Al_2O_3–water nanofluid flow in sinusoidal-wavy channel. Case Stud Therm Eng. 2014;4:153–65.
5. Qi C, Wan Y, Li Ch, Han D, Rao Zh. Experimental and numerical research on the flow and heat transfer characteristics of TiO_2-water nanofluids in a corrugated tube. Int Commun Heat Mass Transfer. 2017;115:1072–84.
6. Zheng W, Li B, Zhang H, You Sh, Li Y, Ye T. Thermal characteristics of a glazed transpired solar collector with perforating corrugated plate in cold regions. Energy. 2016;109:781–90.
7. Greig D, Siddiqui K, Karava P. An experimental investigation of the flow structure over a corrugated waveform in a transpired air collector. Int J Heat Fluid Flow. 2012;38:133–44.
8. El-Sebaii AA, Aboul-Enein S, Ramadan MRI, Shalaby SM, Moharram BM. Investigation of thermal performance of double pass-flat and v-corrugated plate solar air heaters. Energy. 2011;36:1076–86.
9. Caliskan S. Flow and heat transfer characteristics of transverse perforated ribs under impingement jets. Int Commun Heat Mass Transfer. 2013;66:244–60.
10. Aliabadi MKh, Jafari A, Sartipzadeh O, Salami M. Thermal–hydraulic performance of wavy plate-fin heat exchanger using passive techniques: Perforations, winglets, and nanofluids. Int Commun Heat Mass Transfer. 2016;78:231–40.
11. Harleß A, Franz E, Breuer M. Experimental investigation of heat transfer and friction characteristic of fully developed gas flow in single-start and three-start corrugated tubes. Int Commun Heat Mass Transfer. 2016;103:538–47.
12. Wang W, Shuai Y, Ding L, Li B, Sunden B. Investigation of complex flow and heat transfer mechanism in multi-tube heat exchanger with different arrangement corrugated tube. Int J Therm Sci. 2021;167:107010.
13. Laohalertdecha S, Wongwises S. Condensation heat transfer and flow characteristics of R-134a flowing through corrugated tubes. Int Commun Heat Mass Transfer. 2011;54:2673–82.
14. Vicente PG, Garcia A, Viedma A. Experimental investigation on heat transfer and frictional characteristics of spirally corrugated tubes in turbulent flow at different Prandtl numbers. Int Commun Heat Mass Transfer. 2004;47:671–81.
15. Harleß A, Franz E, Breuer M. Heat transfer and friction characteristics of fully developed gas flow in cross-corrugated tubes. Int Commun Heat Mass Transfer. 2017;107:1076–84.
16. Rozzi S, Massini R, Paciello G, Pagliarini G, Rainieri S, Trifiro A, Rozzi S. Heat treatment of fluid foods in a shell and tube heat exchanger: Comparison between smooth and helically corrugated wall tubes. J Food Eng. 2007;79:249–54.
17. Wang W, Zhang Y, Li B, Han H, Gao X. Influence of geometrical parameters on turbulent flow and heat transfer characteristics in outward helically corrugated tubes. Energy Convers Manag. 2017;136:294–306.
18. Córcoles JI, Belmonte JF, Molina AE, Almendros-Ibáñez JA. Influence of corrugation shape on heat transfer performance in corrugated tubes using numerical simulations. Int J Therm Sci. 2019;137:262–75.
19. Xin F, Liu Z, Zheng N, Liu P, Liu W. Numerical study on flow characteristics and heat transfer enhancement of oscillatory flow in a spirally corrugated tube. Int J Heat Mass Transfer. 2018;127:402–13.
20. Dong Y, Huixiong L, Tingkuan C. Pressure drop, heat transfer and performance of single-phase turbulent flow in spirally corrugated tubes. Exp Therm Fluid Sci. 2001;24:131–8.
21. Pethkool S, Eiamsa-ard S, Kwankaomeng S, Promvonge P. Turbulent heat transfer enhancement in a heat exchanger using

helically corrugated tube. In Commun Heat Mass Transfer. 2011;38:340–7.
22. Xiao-wei L, Ji-an M, Zhi-xin L. Roughness enhanced mechanism for turbulent convective heat transfer. Int J Heat Mass Transfer. 2011;54:1775–81.
23. Jaffal HM, Ghani IA, Al-Obaidi AR. The effect of interruptions on thermal characteristics of corrugated tube. Case Stud Therm Eng. 2021;25:100910.
24. Liao W, Luo Y, Chen T. Thermal-hydraulic performance analysis of outward convex corrugated tubes based on skewness and kurtosis. Int J Therm Sci. 2021;165:106970.
25. Sun M, Zeng M. Investigation on turbulent flow and heat transfer characteristics and technical economy of corrugated tube. Appl Therm Eng. 2018;129:1–11.
26. Mohammed HA, Abbas AK, Sheriff JM. Influence of geometrical parameters and forced convective heat transfer in transversely corrugated circular tubes. Int Commun Heat Mass Transfer. 2013;44:116–26.
27. Fan G, Tong P, Sun Z, Chen Y. Experimental study of pure steam and steam–air condensation over a vertical corrugated tube. Prog Nucl Energy. 2018;109:239–49.
28. Huang K, Hu Y, Deng X. Experimental study on heat and mass transfer of falling liquid films in converging-diverging tubes with water. Int J Heat Mass Transfer. 2018;126:721–9.
29. Piroozfam N, Shafaghi AH, Razavi SE. Numerical investigation of three methods for improving heat transfer in counterflow heat exchangers. Int J Therm Sci. 2018;133:230–9.
30. Mirzaei M, Sohankar A, Davidson L, Innings F. Large Eddy Simulation of the flow and heat transfer in a half-corrugated channel with various wave amplitudes. Int J Heat Mass Transfer. 2014;76:432–46.
31. Zhang LY, Duan RJ, Che Y, Lu Z, Cui X, Wei LC, Jin LW. A numerical analysis of fluid flow and heat transfer in wavy and curved wavy channels. Int J Therm Sci. 2022;171:107248.
32. Tsai Y, Liu F, Shen P. Investigations of the pressure drop and flow distribution in a chevron-type plate heat exchanger. Int Commun Heat Mass Transfer. 2009;36:574–8.
33. Faizal M, Ahmed MR. Experimental studies on a corrugated plate heat exchanger for small temperature difference applications. Exp Therm Fluid Sci. 2012;36:242–8.
34. Ma T, Zeng M, Luo T, Chen Y, Wang Q. Numerical study on thermo-hydraulic performance of an offset bubble primary surface channels. Appl Therm Eng. 2013;61:44–52.
35. Hasis F, Krishna PMM, Aravind GP, Deepu M, Shine SR. Thermo hydraulic performance analysis of twisted sinusoidal wavy microchannels. Int J Therm Sci. 2018;128:124–36.
36. Naphon P. Effect of corrugated plates in an in-phase arrangement on the heat transfer and flow developments. Int J Heat Mass Transfer. 2008;51:3963–71.
37. Naphon P, Kornkumjayrit K. Numerical analysis on the fluid flow and heat transfer in the channel with V-shaped wavy lower plate. Int Commun Heat Mass Transfer. 2008;35:839–43.
38. Luo C, Song K, Tagawa T, Wu X, Wang L. Thermal performance of a zig-zag channel formed by two wavy fins. Int J Therm Sci. 2020;153:106361.
39. Islamoglu Y, Parmaksizoglu C. The effect of channel height on the enhanced heat transfer characteristics in a corrugated heat exchanger channel. Appl Therm Eng. 2003;23:979–87.
40. Mohammed HA, Abed AM, Wahid MA. The effects of geometrical parameters of a corrugated channel within out-of-phase arrangement. Int Commun Heat Mass Transfer. 2013;40:47–57.
41. Parlak Z, Parlak N, Islamoglu Y. Optimal design of a converging diverging channel for convective heat transfer enhancement in fully developed turbulent air flow. Int J Therm Sci. 2021;161:106732.
42. Shubham, Saikia A, Dalal A, Pati S. Thermo-hydraulic transport characteristics of non-Newtonian fluid flows through corrugated channels. Int J Therm Sci. 2018;129:201–208.
43. Wang CC, Chen CK. Forced convection in a wavy-wall channel. Int J Heat Mass Transfer. 2002;45:2587–95.
44. Pehlivan H. Experimental investigation of convection heat transfer in converging-diverging wall channels. Int J Heat Mass Transfer. 2013;66:128–38.
45. Taymaz I, Koc I, Islamoglu Y. Experimental study on forced convection heat transfer characteristics in a converging diverging heat exchanger channel. Heat Mass Transfer. 2008;44:1257–62.
46. Gong L, Kota K, Tao W, Joshi Y. Parametric Numerical Study of Flow and Heat Transfer in Microchannels with Wavy Walls. J Heat Transfer. 2011;133:1–10.
47. Pourhammati S, Hossainpour S. Improving the hydrothermal characteristics of wavy microchannel heat sink by modification of wavelength and wave amplitude. Int Commun Heat Mass Transfer. 2022;130:105805.
48. Rostami J, Abbassi A, Saffar-Avval M. Optimization of conjugate heat transfer in wavy walls microchannels. Appl Therm Eng. 2015;82:318–28.
49. Mohammed HA, Gunnasegaran P, Shuaib NH. Numerical simulation of heat transfer enhancement in wavy microchannel heat sink. Int Commun Heat Mass Transfer. 2011;38:63–8.
50. Mohammed HA, Gunnasegaran P, Shuaib NH. Influence of channel shape on the thermal and hydraulic performance of microchannel heat sink. Int Commun Heat Mass Transfer. 2011;38:474–80.
51. Yong JQ, Teo CJ. Mixing and heat transfer enhancement in microchannels containing Converging-Diverging Passages. J Heat Transfer. 2014;136:1–11.
52. Wan Z, Lin Q, Wang X, Tang Y. Flow characteristics and heat transfer performance of half-corrugated microchannels. Appl Therm Eng. 2017;123:1140–51.
53. Sui Y, Lee PS, Teo CJ. An experimental study of flow friction and heat transfer in wavy microchannels with rectangular cross section. Int J Therm Sci. 2011;50:2473–82.
54. Ermagan H, Rafee R. Numerical investigation into the thermo-fluid performance of wavy microchannels with superhydrophobic walls. Int J Therm Sci. 2018;132:578–88.
55. Lin L, Zhao J, Lu G, Wang X, Yan W. Heat transfer enhancement in microchannel heat sink by wavy channel with changing wavelength/amplitude. Int J Therm Sci. 2017;118:423–34.
56. Chiam Z, Lee PS, Singh PK, Moua N. Investigation of fluid flow and heat transfer in wavy micro-channels with alternating secondary branches. Int J Heat Mass Transfer. 2016;101:1316–30.
57. Aliabadi MKh, Deldar S, Salimi A, Rashidi MM. Effects of cross-section geometry on performance of corrugated miniature heat sink: Uniform, convergent, divergent, and hybrid cases. Int J Heat Mass Transfer. 2021;127:105269.
58. Aliabadi MKh, Nozan F. Water cooled corrugated minichannel heat sink for electronic devices: Effect of corrugation shape. Int J Heat Mass Transfer. 2016;76:188–96.
59. Aliabadi MKh, Sahamiyan M. Performance of nanofluid flow in corrugated minichannels heat sink (CMCHS). Energy Convers Manage. 2016;108:297–308.
60. Aliabadi MKh, Hassani SM, Mazloumi SH. Performance enhancement of straight and wavy miniature heat sinks using pin-fin interruptions and nanofluids. Chem Eng Process: Process Intensif. 2017;122:90–108.
61. Aliabadi MKh, Sahamiyan M, Hesampour M, Sartipzadeh O. Experimental study on cooling performance of sinusoidal–wavy minichannel heat sink. Appl Therm Eng. 2016;92:50–61.
62. Khalifa MA, Jaffal HM. Effects of Channel Configuration on Hydrothermal Performance of the Cylindrical Mini-channel Heat Sinks. Appl Therm Eng. 2019;148:1107–30.

63. Abdullah AS, Omara ZM, Essa FA, Younes MM, Shanmugan S, Abdelgaied M, Amro MI, Kabeel AE, Farouk WM. Improving the performance of trays solar still using wick corrugated absorber, nano-enhanced phase change material and photovoltaics-powered heaters. J Energy Storage. 2021;40:102782.
64. Younes MM, Abdullah AS, Essa FA, Omara ZM, Amro MI. Enhancing the wick solar still performance using half barrel and corrugated absorbers. Process Saf Environ Prot. 2021;15:440–52.
65. Aboghrara AM, Baharudin BTHT, Alghoul MA, Adam NM, Hairuddin AA, Hasan HA. Performance analysis of solar air heater with jet impingement on corrugated absorber plate. Case Stud Therm Eng. 2017;10:111–20.
66. Taha SY, Farhan AA. Performance augmentation of a solar air heater using herringbone metal foam fins: An experimental work. Int J Energy Res. 2021;45:2321–33.
67. Dormohammadi R, Farzaneh-Gord M, Ebrahimi-Moghadam A, Ahmadi MH. Heat transfer and entropy generation of the nanofluid flow inside sinusoidal wavy channels. J Mol Liq. 2018;269:229–40.
68. Pavlovic S, Bellos E, Loni R. Exergetic investigation of a solar dish collector with smooth and corrugated spiral absorber operating with various nanofluids. J Cleaner Prod. 2018;174:1147–60.
69. Kumar R, Chand P. Performance enhancement of solar air heater using herringbone corrugated fins. J Energy. 2017;127:271–9.
70. Zheng W, Zhang H, You Sh, Fu Y, Zheng X. Thermal performance analysis of a metal corrugated packing solar air collector in cold regions. Appl Energy. 2017;203:938–47.
71. Álvarez A, Tarrío-Saavedra J, Zaragoza S, López-Beceiro J, Artiaga R, Naya S, Álvarez B. Numerical and experimental study of a corrugated thermal collector. Case Stud Therm Eng. 2016;8:41–50.
72. Joudi KA, Farhan AA. Greenhouse heating by solar air heaters on the roof. Renew Energy. 2014;72:406–14.
73. Kumar PG, K. Panchabikesan K, Deeyoko LAJ, Ramalingam V. Experimental investigation on heat transfer augmentation of solar air heater using shot blasted V-corrugated absorber plate. Renewable Energy. 2018;127:213–229.
74. Zhang D, Li J, Gao Zh, Wang L, Nan J. Thermal Performance Investigation of Modified Flat Plate Solar Collector with Dual-Function. Appl Therm Eng. 2016;108:1126–35.
75. Hedayatizadeh M, Ajabshirchi Y, Sarhaddi F, Farahat S, Safavinejad A, Chaji H. Analysis of exergy and parametric study of a v-corrugated solar air heater. Heat Mass Transfer. 2012;48:1089–101.
76. Ho Ch, Hsiao Ch, Chang H, Tien Y. Investigation of device performance for recycling double-pass V-corrugated solar air collectors. Energy Procedia. 2017;105:28–34.
77. Hedayatizadeh M, Sarhaddi F, Safavinejad A, Ranjbar F, Chaji H. Exergy loss-based efficiency optimization of a double-pass/glazed v-corrugated plate solar air heater. Energy. 2016;94:799–810.
78. Karim MA, Hawlader MNA. Performance investigation of flat plate, v-corrugated and finned air collectors. Energy. 2006;31:452–70.
79. A.A. Farhan AA, I.M.I. Aljubury IMI, H.E. Ahmed HE. Energetic and exergetic efficiency analysis of a v-corrugated solar air heater integrated with twisted tape inserts. Renewable Energy. 2021;169:1373–1385,
80. Liu T, Lin W, Gao W, Xia C. A comparative study of the thermal performances of cross-corrugated and v-groove solar air collectors. Int J Green Energy. 2007;4:427–45.
81. Akbarzadeh M, Rashidi S, Karimi N, Ellahi R. Convection of heat and thermodynamic irreversibilities in two-phase, turbulent nanofluid flows in solar heaters by corrugated absorber plates. 2018;29:2243–2254
82. Rainieri S, Pagliarini G. Convective heat transfer to temperature dependent property fluids in the entry region of corrugated tubes. Int J Heat Mass Transfer. 2002;45:4525–36.
83. Islamoglu Y. Effect of rounding of protruding edge on convection heat transfer in a converging-diverging channel. Int J Heat Mass Transfer. 2008;35:643–7.
84. Nelly SM, Nieratschker W, Nadler M, Raab D, Delgado A. Experimental and numerical investigation of the pressure drop and heat transfer coefficient in corrugated tubes. Chem Eng Technol. 2015;38:2279–90.
85. Dizaji HS, Jafarmadar S, Mobadersani F. Experimental studies on heat transfer and pressure drop characteristics for new arrangements of corrugated tubes in a double pipe heat exchanger. Int J Therm Sci. 2015;96:211–20.
86. Elshafei EAM, Awad MM, El-Negiry E, Ali AG. Heat transfer and pressure drop in corrugated channels. Energy. 2010;35:101–10.
87. Bilen K, Cetin M, Gul H, Balta T. The investigation of groove geometry effect on heat transfer for internally grooved tubes. Appl Therm Eng. 2009;29:753–61.
88. Han H, Li B, Yu B, He Y, Li F. Numerical study of flow and heat transfer characteristics in outward convex corrugated tubes. Int J Heat Mass Transfer. 2012;55:7782–802.
89. Wang W, Zhang Y, Li B, Li Y. Numerical investigation of tube-side fully developed turbulent flow and heat transfer in outward corrugated tubes. Int J Heat Mass Transfer. 2018;116:115–26.
90. Du J, Hong Y, Huang S, Ye W, Wang Sh. Laminar thermal and fluid flow characteristics in tubes with sinusoidal ribs. Int J Heat Mass Transfer. 2018;120:635–51.
91. Hong Y, Du J, Wang S, Huang S. Heat transfer and flow behaviors of a wavy corrugated tube. Appl Therm Eng. 2017;126:151–66.
92. Zhang L, Che D. Influence of corrugation profile on the thermal-hydraulic performance of cross-corrugated plates. Numer Heat Transfer, Part A. 2011;59:267–96.
93. Ferley DM, Ormiston SJ. Numerical analysis of laminar forced convection in corrugated-plate channels with sinusoidal, ellipse, and rounded-vee wall shapes. Numer Heat Transfer, Part A. 2013;63:563–89.
94. Bahaidarah HMS, Anand NK, Chen HC. Numerical study of heat and momentum transfer in channels with wavy walls. Numer Heat Transfer, Part A. 2005;47:417–39.
95. Hassan H, Yousef MS, Abo-Elfadl S. Energy, exergy, economic and environmental assessment of double pass V-corrugated-perforated finned solar air heater at different air mass ratios. Sustainable Energy Technol Assess. 2021;43:100936.
96. Zhang H, Ma X, You Sh, Wang Y, Zheng X, Ye T, Zheng W, Wei Sh. Mathematical modeling and performance analysis of a solar air collector with slit-perforated corrugated plate. Sol Energy. 2018;167:147–57.
97. Aliabadi MKh, Tatari M, Salami M. Analysis on Al2O3/water nanofluid flow in a channel by inserting corrugated/perforated fins for solar heating heat exchangers. Renew Energy. 2018;115:1099–108.
98. Ameri M, Sardari R, Farzan H. Thermal performance of a V-corrugated serpentine solar air heater with integrated PCM: a comparative experimental study. Renew Energy. 2021;171:391–400.
99. Kabeel AE, Khalil A, Shalaby SM, Zayed ME. Experimental investigation of thermal performance of flat and v-corrugated plate solar air heaters with and without PCM as thermal energy storage. Energy Convers Manag. 2016;113:264–72.
100. Kh. Aliabadi MKh. Influence of different design parameters and Al_2O_3-water nanofluid flow on heat transfer and flow characteristics of sinusoidal-corrugated channels. Energy Convers Manag. 2014;88:96–105.
101. Wang G, Qi C, Liu M, Li Ch, Yan Y, Liang L. Effect of corrugation pitch on thermo-hydraulic performance of nanofluids

in corrugated tubes of heat exchanger system based on exergy efficiency. Energy Convers Manag. 2019;186:51–65.
102. Ajeel RK, Salim W, Hasnan Kh. Design characteristics of symmetrical semicircle-corrugated channel on heat transfer enhancement with nanofluid. Int J Mech Sci. 2019;151:236–50.
103. Ahmed MA, Shuaib NH, Yusoff MZ, Al-Falahi AH. Numerical investigations of flow and heat transfer enhancement in a corrugated channel using nanofluid. Int Commun Heat Mass Transfer. 2011;38:1368–75.
104. Ahmed MA, Shuaib NH, Yusoff MZ. Numerical investigations on the heat transfer enhancement in a wavy channel using nanofluid. Int Commun Heat Mass Transfer. 2012;55:5891–8.
105. Ahmed MA, Yusoff MZ, Ng KC, Shuaib NH. Effect of corrugation profile on the thermal–hydraulic performance of corrugated channels using CuO–water nanofluid. Case Stud Therm Eng. 2014;4:65–75.
106. Ahmed MA, Yusoff MZ, Ng KC, Shuaib NH. Numerical and experimental investigations on the heat transfer enhancement in corrugated channels using SiO_2– water nanofluid. Case Stud Therm Eng. 2015;6:77–92.
107. Goodarzi M, Amiri A, Goodarzi MSh, Safaei MR, Karimipour A, Languri EM, Dahari M. Investigation of heat transfer and pressure drop of a counter flow corrugated plate heat exchanger using MWCNT based nanofluids. Int Commun Heat Mass Transfer. 2015;66:172–9.
108. Naphon P, Wiriyasart S. Pulsating flow and magnetic field effects on the convective heat transfer of TiO_2-water nanofluids in helically corrugated tube. Int Commun Heat Mass Transfer. 2018;125:1054–60.
109. Mei S, Qi C, Luo T, Zhai X, Yan Y. Effects of magnetic field on thermo-hydraulic performance of Fe_3O_4-water nanofluids in a corrugated tube. Int Commun Heat Mass Transfer. 2019;128:24–45.

Publisher's Note Springer Nature remains neutral with regard to jurisdictional claims in published maps and institutional affiliations.